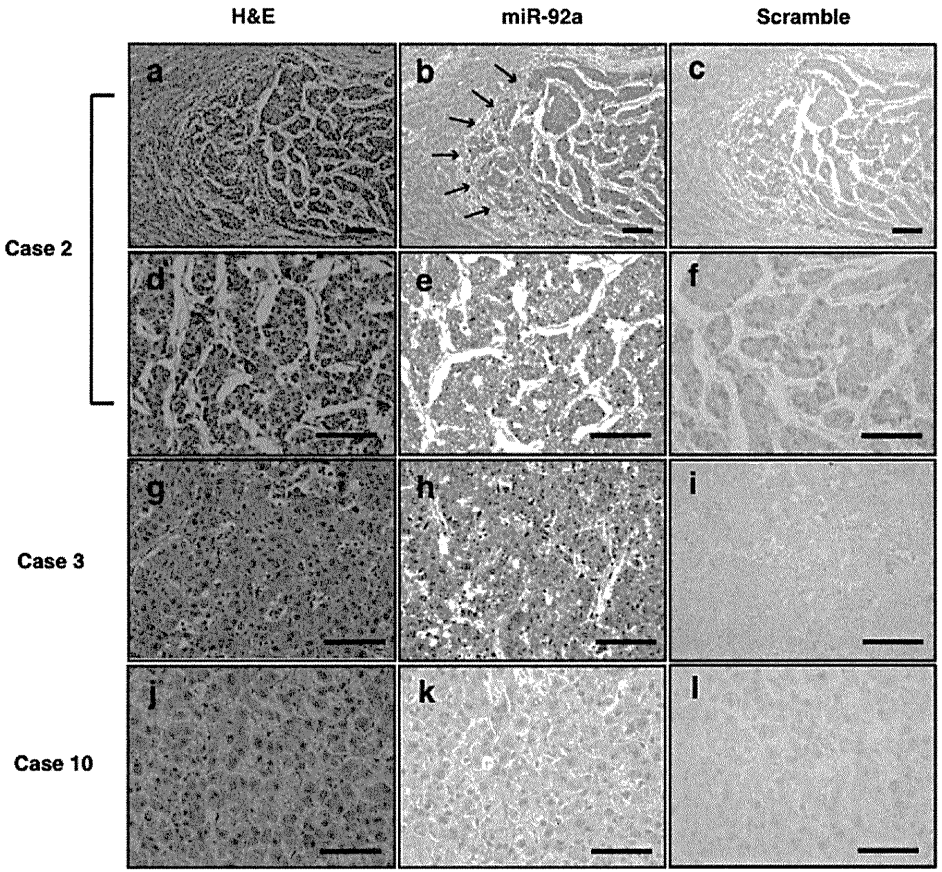

Figure 1 MiRNA expression in hepatocellular carcinoma (HCC). *In situ* hybridization was performed using Locked nucleic acid (LNA)-modified probes for miR-92a and negative control. Case 2 and Case 3 were positive cases for miR-92a. Case 10 was a negative case for miR-92a. (**a–c**) Low power field of boundary of HCC and non-tumor lesion. Arrowheads indicated a border. Only HCC regions were positive for miR-92a. (**d–l**) High power field of HCC. Blue signals represent positive for miR-92a. Bars indicate 100 μm.

plasma was isolated using Isogen-LS (NIPPON GENE, Tokyo, Japan) according to the manufacturer's instructions. The RNA sample was suspended in 20 μL of nuclease free water. In general, we obtained 400 ng of RNA from 1 mL of plasma. MiRNAs were quantified using TaqMan MiRNA Assays (Applied Biosystems, Life Technologies Corporation, Carlsbad, CA, USA) as previously described.[13]

For miR-92a quantification in tissue samples, five pairs of fresh HCC and non-tumorous LC samples were surgically resected from HCC patients (Table 2). All the patients or their guardians provided written informed consent, and the Ethics Committee of the Kyoto University Graduate School and Faculty of Medicine approved all aspects of this study. The amounts of miR-92a were normalized to RNU48 that is one of rRNAs (Applied Biosystems).

Cell culture and transfection

Hepatocellular carcinoma (HCC) cell lines HepG2, OR6 and SN1a were cultured in Dulbecco's modified Eagle's medium

(DMEM) (Sigma, St. Louis, MO, USA) supplemented with 10% fetal bovine serum (FBS). OR6 and SN1a are derived from the Huh7 HCC cell line and maintain hepatitis C virus (HCV) replicon.[14–16] The miR-92a oligonucleotide used in the transfection experiments is a synthetic double-strand 19 nucleotide RNA oligonucleotide (5′-UUGCACUUGUCCC GGCCUG-3′) purchased from B-Bridge International (Tokyo, Japan). The scrambled oligonucleotide represents a mix of two different frames of the miR-92 sequence (5′-UAUUGC ACUUGUCCCGGCCUGUCCCGGCC-3′ and 5′-AUUGCAC UUGUCCCGGCCUTT-3′). Locked nucleic acid (LNA) oligonucleotide miR-92 knockdown (antagomir) was obtained from Exiqon (Vedbaek, Denmark, http://www.exiqon.com). The oligonucleotides were individually transfected by HiperFect (QIAGEN K. K., Tokyo, Japan) into the cells at a final concentration of 100 nM.

In vitro proliferation assays

The effects of miR-92a and the anti-miR-92a antagomir on the growth of HepG2, OR6 and SN1a were evaluated using the MTT cell growth assay kit (Cell Count Reagent SF, Nacalai tesque, Kyoto, Japan). The cells were transfected with miR-92a or the antagomir. The cell numbers were then assessed with MTT assay at 48 or 72 h after the transfection. The MTT assay was performed according to the manufacturer's recommendation. The reagents were added to each well and incubated at 37°C for 4 h. The MTT reduced by living cells into a formazan product was assayed with a multiwell scanning spectrophotometer at 450 nm.

RESULTS

Highly expression of miR-92a in HCC cells

We first examined whether or not miR-92a is expressed in hepatocellular carcinoma (HCC). We performed *in situ* hybridization using locked nucleic acid (LNA)-modified probes digoxigenin (DIG) labelled. We found that miR-92a was strongly expressed in cancer cells of 17 out of 22 HCC cases (Table 1 and Fig. 1). No significant differences were observed in age, sex, virus type, clinical stage and tumor differentiation of the clinical samples. In contrast, we did not detect miR-92a expression in non-cancerous hepatocytes around the HCCs.

Furthermore, we quantified miR-92a levels in HCC sections ($n = 5$) and their adjacent non-tumorous liver cirrhosis (LC) sections ($n = 5$) by *Taq*Man qRT-PCR (Table 2 and Fig. 2). The levels of miR-92a expression in HCC sections were higher than that in adjacent LC sections (Fig. 2).

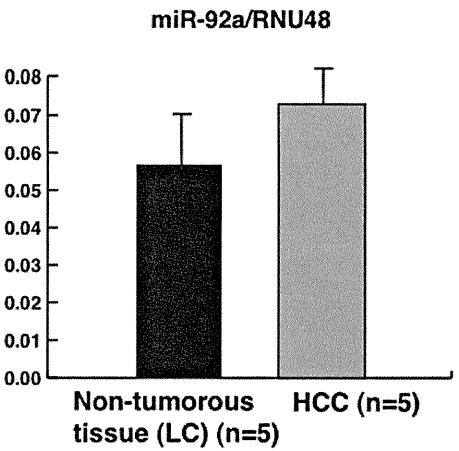

Figure 2 Quantification of miR-92a expression in hepatocellular carcinoma (HCC) tissue samples. The ratios of miR-92a to RNU48 in HCC tissues and their adjacent non-tumorous liver cirrhosis (LC) tissues were analyzed by *Taq*Man qRT-PCR. *Bars*, s.d.

Effects of miR-92a on a Hepatoma cell lines HepG2, OR6 and SN1a

Next, we investigated whether miR-92a affects cell proliferation of human HCC cell lines, HepG2, OR6 and SN1a. We transiently transfected either miR-92a or the anti-miR-92a antagomir into the cells. Antagomirs are single-stranded RNAs that are complementary to a specific miRNA and cause the depletion of the miRNA.[17] After the transfection, we found that all of the cells transfected with the anti-miR-92a antagomir showed lower proliferation rate than the cells transfected with a control RNA oligonucleotide (Fig. 3a). In contrast, the cells except for HepG2 showed increased proliferation rate when miR-92a was transfected (Fig. 3a). We also confirmed the amounts of miR-92a in the cells by quantitative real time PCR (Fig. 3b).

The ratio of miR-92a to miR-638 serves as a biomarker for HCC

Finally, we sought to determine whether the expression level of miR-92a in blood sera could discriminate HCC patients from healthy individuals. Previously, we have revealed that miR-92a is dramatically reduced in the plasmas of acute leukemia patients although in leukemic cells it is strongly expressed.[13] We analyzed the miR-92a levels in the plasma samples from normal individuals ($n = 10$) and HCC patients

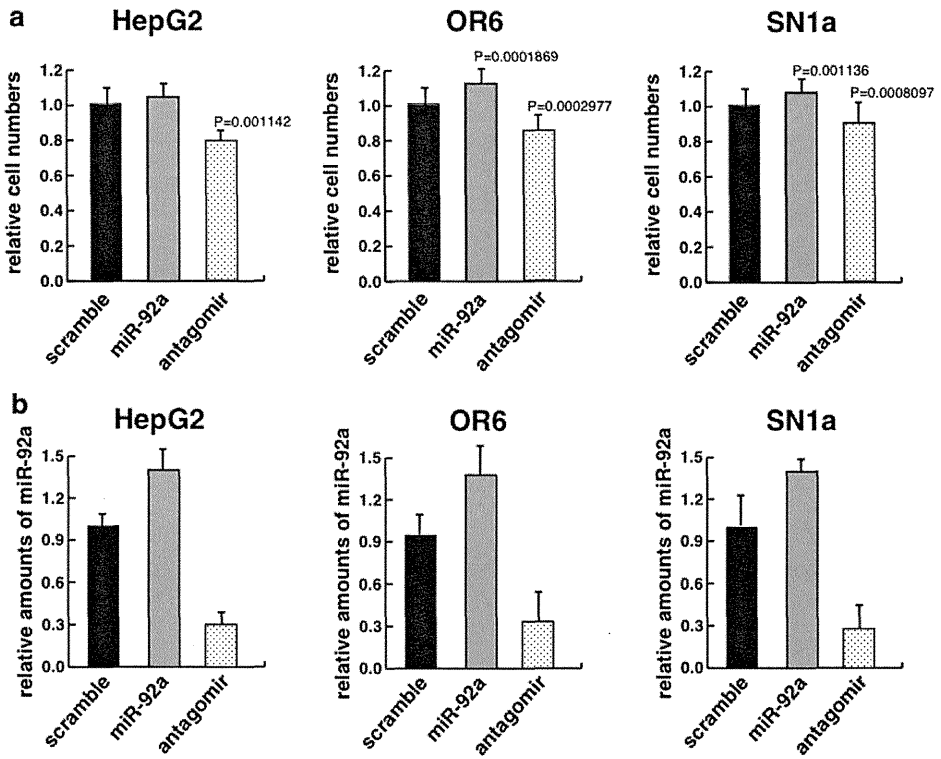

Figure 3 miR-92a modulates proliferation of HepG2, OR6 and SN1a cells. (**a**) Cell numbers of the HepG2, OR6 and SN1a cells transfected with synthetic miR-92a, anti-miR-92a antagomir, or scrambled control oligonucleotide were analyzed by MTT assays at 48 h for OR6 and SN1a and 72 h for HepG2 after transfection. *Bars*, s.d. (**b**) qRT-PCR analysis of miR-92a amounts in the cells transfected with miR-92a, anti-miR-92a antagomir or scrambled control at 48 h for OR6 and SN1a and 72 h for HepG2 after the transfection.

(n = 10) by *Taq*Man qRT-PCR. Because miR-638 is stably present in human plasmas,[13] we used miR-638 as the standard to improve the precision of the data. The ratio of miR-92a to miR-638 in the plasma samples from the HCC patients were decreased compared with that from the normal donors (Fig. 4a). Then, we further examined the ratio from the patients after surgical resection. Interestingly, the miR-92a/miR-638 levels were significantly higher than that in the plasmas from the patients before surgical resection (Fig. 4b).

DISCUSSION

In this study, we found that miR-92a was highly expressed in HCC (Figs 1,2). In addition, we demonstrated that the expression level of miR-92a affects the proliferation of hepatoma cell lines, HepG2, OR6 and SN1a (Fig. 3). These results suggest that miR-92a may play an important role in tumor progression of hepatocyte. We do not know why, but addition of miR-92a did not significantly increase the proliferation of HepG2 cells. It may be possible that HepG2 cells themselves already contain enough miR-92a to promote cancer cell proliferation. In addition, miR-92a is a part of the miR-17-92 cluster, which is actively involved in the development and progression of various cancers.[4–10] However, the molecular function of miR-92a is still unknown, and its mRNA targets have not been identified. Recently, it has been shown that one of the molecular mechanisms through which miR-92a increases cell proliferation is by negative regulation of an isoform of the cell-cycle regulator p63.[11] Thus, we examined

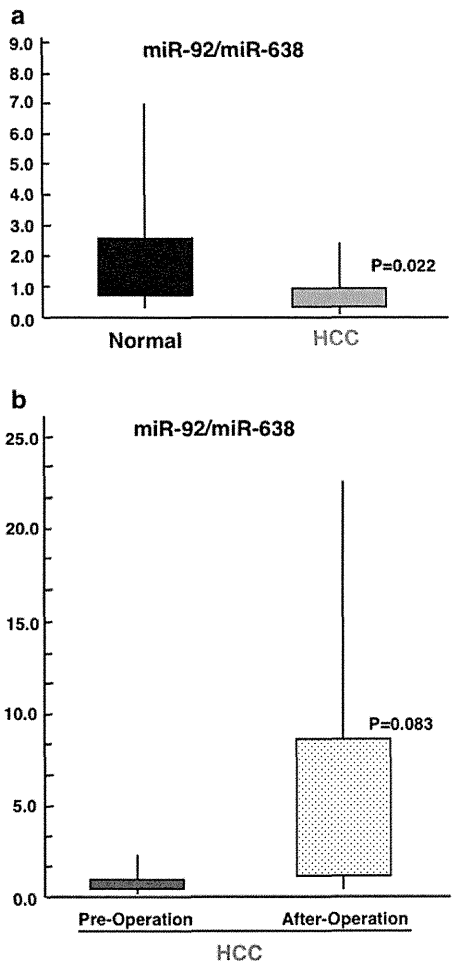

Figure 4 Comparison of miR-92a levels in the plasmas from normal individuals and hepatocellular carcinoma (HCC) patients. (**a**) The ratios of miR-92a to miR-638 in the plasmas from normal donors and HCC patients were analyzed by *Taq*Man qRT-PCR. Student's *t*-test was used to determine statistical significance. (**b**) The ratios of miR-92a to miR-638 in the plasmas from HCC patients before and after tumor resection were analyzed by *Taq*Man qRT-PCR.

the expression of p63 in HCC by immunohistochemistry. However, we could not find the positive nuclear staining both in HCC and normal hepatocyte (data not shown). On the other hand, the miRanda software found 300 different genes that have putative miR-92a binding sites conserved among *Homo sapiens*, *Mus musculus*, and *Rattus norvegicus* at the 3′-UTR regions of their transcripts. Therefore, at least in HCC, there may be novel miR-92a targets that are involved in cancer cell proliferation.

In this report, we have revealed that the value of miR-92a/miR-638 in plasma has potential as a very sensitive marker for HCC. We found that the ratio of miR-92a to miR-638 in the plasma samples from the HCC patients were decreased compared with that from the normal donors (Fig. 4a). We did not find any differences in the values of the ratios between hepatitis B virus (HBV) infection and hepatitis C virus (HCV) infection (data not shown). On the other hand, we recently observed decrease of miR-92a in plasma samples of acute leukemia.[13] These results suggest that the decrease of the miR-92a/miR-638 level in human plasma may serve as a valuable diagnostic marker for not only acute leukemia but also solid tumors such as HCC. Moreover, we observed increase of miR-92a/miR-638 levels in the plasmas from the HCC patients after tumor resection (Fig. 4b). Thus, the miR-92a/miR-638 levels in human plasmas may also be a potential noninvasive follow up marker of HCC. To confirm this notion, a large number of plasma samples should be examined. Nevertheless, the levels of miR-92a/miR-638 promise to be an effective biomarker for malignant tumors. The physiological significance of the decrease of miR-92a in plasma is still unknown.

In summary, we have shown that miR-92a may be involved in HCC development. In addition, we have demonstrated that the ratio of miR-92a/miR-638 in blood is expected to be useful for diagnosis of HCC patients. This study may also provide useful information for further investigations of functional association between miRNAs and HCC.

ACKNOWLEDGMENTS

This work was supported by Grants-in-Aids from the Ministry of Education, Culture, Sports, Science and Technology of Japan, the Ministry of Health, Labour and Welfare of Japan, Japan Health Sciences Foundation and a grant of Yamaguchi Endocrine Research Association and the grant of 'University-Industry Joint Research Project' for private universities as well as a matching fund subsidy from the MEXT (Ministry of Education, Culture, Sports, Science and Technology, 2007–2009). We thank Koji Fujita for his technical assistance and Satoko Aochi for her outstanding editorial assistance.

REFERENCES

1 Mattick JS, Makunin IV. Non-coding RNA. *Hum Mol Genet* 2006; **15** (Spec No. 1): R17–29.

2 Esquela-Kerscher A, Slack FJ. Oncomirs—microRNAs with a role in cancer. *Nat Rev Cancer* 2006; **6**: 259–69.
3 Osada H, Takahashi T. MicroRNAs in biological processes and carcinogenesis. *Carcinogenesis* 2007; **28**: 2–12.
4 Hayashita Y, Osada H, Tatematsu Y *et al.* A polycistronic microRNA cluster, miR-17-92, is overexpressed in human lung cancers and enhances cell proliferation. *Cancer Res* 2005; **65**: 9628–32.
5 He L, Thomson JM, Hemann MT *et al.* A microRNA polycistron as a potential human oncogene. *Nature* 2005; **435**: 828–33.
6 Venturini L, Battmer K, Castoldi M *et al.* Expression of the miR-17-92 polycistron in chronic myeloid leukemia (CML) CD34+ cells. *Blood* 2007; **109**: 4399–405.
7 Uziel T, Karginov FV, Xie S *et al.* The miR-17-92 cluster collaborates with the Sonic Hedgehog pathway in medulloblastoma. *Proc Natl Acad Sci USA* 2009; **106**: 2812–17.
8 Diosdado B, van de Wiel MA, Terhaar Sive Droste JS *et al.* MiR-17-92 cluster is associated with 13q gain and c-myc expression during colorectal adenoma to adenocarcinoma progression. *Br J Cancer* 2009; **101**: 707–14.
9 Connolly E, Melegari M, Landgraf P *et al.* Elevated expression of the miR-17-92 polycistron and miR-21 in hepadnavirus-associated hepatocellular carcinoma contributes to the malignant phenotype. *Am J Pathol* 2008; **173**: 856–64.
10 Ventura A, Young AG, Winslow MM *et al.* Targeted deletion reveals essential and overlapping functions of the miR-17 through 92 family of miRNA clusters. *Cell* 2008; **132**: 875–86.
11 Manni I, Artuso S, Careccia S *et al.* The microRNA miR-92 increases proliferation of myeloid cells and by targeting p63 modulates the abundance of its isoforms. *FASEB J* 2009; **23**: 3957–66.
12 Bonauer A, Carmona G, Iwasaki M *et al.* MicroRNA-92a controls angiogenesis and functional recovery of ischemic tissues in mice. *Science* 2009; **324**: 1710–13.
13 Tanaka M, Oikawa K, Takanashi M *et al.* Down-regulation of miR-92 in human plasma is a novel marker for acute leukemia patients. *PLoS ONE* 2009; **4**: e5532.
14 Lohmann V, Korner F, Koch J, Herian U, Theilmann L, Bartenschlager R. Replication of subgenomic hepatitis C virus RNAs in a hepatoma cell line. *Science* 1999; **285**: 110–13.
15 Ikeda M, Abe K, Dansako H, Nakamura T, Naka K, Kato N. Efficient replication of a full-length hepatitis C virus genome, strain O, in cell culture, and development of a luciferase reporter system. *Biochem Biophys Res Commun* 2005; **329**: 1350–9.
16 Ikeda M, Abe K, Yamada M, Dansako H, Naka K, Kato N. Different anti-HCV profiles of statins and their potential for combination therapy with interferon. *Hepatology* 2006; **44**: 117–25.
17 Krutzfeldt J, Rajewsky N, Braich R *et al.* Silencing of microRNAs in vivo with 'antagomirs'. *Nature* 2005; **438**: 685–9.

OPEN ACCESS Freely available online PLoS one

The Progression of Liver Fibrosis Is Related with Overexpression of the miR-199 and 200 Families

Yoshiki Murakami[1]*, Hidenori Toyoda[2], Masami Tanaka[3], Masahiko Kuroda[3], Yoshinori Harada[4], Fumihiko Matsuda[1], Atsushi Tajima[5¤], Nobuyoshi Kosaka[6], Takahiro Ochiya[6], Kunitada Shimotohno[7]

1 Center for Genomic Medicine, Kyoto University Graduate School of Medicine, Kyoto, Japan, **2** Department of Gastroenterology, Ogaki Municipal Hospital, Ogaki, Japan, **3** Department of Molecular Pathology, Tokyo Medical University, Tokyo, Japan, **4** Department of Pathology and Cell Regulation, Kyoto Prefectural University of Medicine, Kyoto, Japan, **5** Department of Molecular Life Science, Tokai University School of Medicine, Isehara, Japan, **6** Division of Molecular and Cellular Medicine, National Cancer Center Research Institute, Tokyo, Japan, **7** Research Institute, Chiba Institute of Technology, Narashino, Japan

Abstract

Background: Chronic hepatitis C (CH) can develop into liver cirrhosis (LC) and hepatocellular carcinoma (HCC). Liver fibrosis and HCC development are strongly correlated, but there is no effective treatment against fibrosis because the critical mechanism of progression of liver fibrosis is not fully understood. microRNAs (miRNAs) are now essential to the molecular mechanisms of several biological processes. In order to clarify how the aberrant expression of miRNAs participates in development of the liver fibrosis, we analyzed the liver fibrosis in mouse liver fibrosis model and human clinical samples.

Methodology: In a CCl_4-induced mouse liver fibrosis model, we compared the miRNA expression profile from CCl_4 and olive oil administrated liver specimens on 4, 6, and 8 weeks. We also measured expression profiles of human miRNAs in the liver biopsy specimens from 105 CH type C patients without a history of anti-viral therapy.

Principle Findings: Eleven mouse miRNAs were significantly elevated in progressed liver fibrosis relative to control. By using a large amount of human material in CH analysis, we determined the miRNA expression pattern according to the grade of liver fibrosis. We detected several human miRNAs whose expression levels were correlated with the degree of progression of liver fibrosis. In both the mouse and human studies, the expression levels of miR-199a, 199a*, 200a, and 200b were positively and significantly correlated to the progressed liver fibrosis. The expression level of fibrosis related genes in hepatic stellate cells (HSC), were significantly increased by overexpression of these miRNAs.

Conclusion: Four miRNAs are tightly related to the grade of liver fibrosis in both human and mouse was shown. This information may uncover the critical mechanism of progression of liver fibrosis. miRNA expression profiling has potential for diagnostic and therapeutic applications.

Citation: Murakami Y, Toyoda H, Tanaka M, Kuroda M, Harada Y, et al. (2011) The Progression of Liver Fibrosis Is Related with Overexpression of the miR-199 and 200 Families. PLoS ONE 6(1): e16081. doi:10.1371/journal.pone.0016081

Editor: Chad Creighton, Baylor College of Medicine, United States of America

Received September 15, 2010; **Accepted** December 6, 2010; **Published** January 24, 2011

Funding: This work was supported by the Japanese Ministry of Health, Labour and Welfare (Y.M, and K.S). This work was also supported by the 'Strategic Research-Based Support' Project for private universities; with matching funds from the Ministry of Education, Culture, Sports, Science and Technology (M.K). The funders had no role in study design, data collection and analysis, decision to publish, or preparation of the manuscript.

Competing Interests: The authors have declared that no competing interests exist.

* E-mail: ymurakami@genome.med.kyoto-u.ac.jp

¤ Current address: Department of Human Genetics and Public Health, Institute of Health Biosciences, The University of Tokushima Graduate School, Tokushima, Japan

Introduction

Chronic viral hepatitis is a major risk factor for hepatocellular carcinoma (HCC) [1]. Worldwide 120–170 million persons are currently chronically Hepatitis C Virus (HCV) infected [2]. Due to repetitive and continuous inflammation, these patients are at increased risk of developing cirrhosis, subsequent liver decompensation and/or hepatocellular carcinoma. However, the current standard of care; pegylated interferon and rivabirin combination therapy is unsatisfied in the patients with high titre of HCVRNA and genotype 1b. Activated human liver stellate cells (HSC) with chronic viral infection, can play a pivotal role in the progression of liver fibrosis [3]. Activated HSC produce a number of profibrotic cytokines and growth factors that perpetuate the fibrotic process through paracrine and autocrine effects.

MicroRNAs (miRNAs) are endogenous small non-coding RNAs that control gene expression by degrading target mRNA or suppressing their translation [4]. There are currently 940 identifiable human miRNAs (The miRBase Sequence Database - Release ver. 15.0). miRNAs can recognize hundreds of target genes with incomplete complementary; over one third of human genes appear to be conserved miRNA targets [5][6]. miRNA is associated several pathophysiologic events as well as fundamental cellular processes such as cell proliferation and differentiation. Aberrant expression of miRNA can be associated with the liver diseases [7][8][9][10]. Recently reported miRNAs can regulate the activation of HSCs and thereby regulate liver fibrosis. miR-29b, a negative regulator for the type I collagen and SP1, is a key regulator of liver fibrosis [11]. miR-27a and 27b allowed culture-activated rat HSCs to switch to a more quiescent HSC phenotype,

with restored cytoplasmic lipid droplets and decreased cell proliferation [12].

In this study, we aimed to reveal the association between miRNA expression patterns and the progression of liver fibrosis by using a chronic liver inflammation model in mouse. We also sought to identify the miRNA expression profile in chronic hepatitis (CH) C patients according to the degree of liver fibrosis, and to clarify how miRNAs contribute to the progression of liver fibrosis. We observed a characteristic miRNA expression profile common to both human liver biopsy specimens and mouse CCL_4 specimens, comprising the key miRNAs which are associated with the liver fibrosis. This information is expected to uncover the mechanism of liver fibrosis and to provide a clearer biomarker for diagnosis of liver fibrosis as well as to aid in the development of more effective and safer therapeutic strategies for liver fibrosis.

Results

The expression level of several mouse miRNAs was increased by introducing mouse liver fibrosis

In order to identify changes in the miRNA expression profile between advanced liver fibrosis and non-fibrotic liver, we intraperitoneally administered CCL_4 in olive oil or olive oil alone twice a week for 4 weeks and then once a week for the next 4 weeks. Mice were sacrificed at 4, 6, or 8 weeks and then the degree of mouse liver fibrosis was determined by microscopy (Figure S1). miRNA expression analysis was performed from the liver tissue collected at the same time. Histological examination revealed that the degree of liver fibrosis progressed in mice that received CCL_4 relative to mice receiving olive oil alone (Figure 1A). Microarray analysis revealed that in CCL_4 mice, the expression level of 11 miRNAs was consistently higher than that in control mice (Figure 1B).

miRNA expression profile in each human liver fibrosis grade

We then established human miRNAs expression profile by using 105 fresh-frozen human chronic hepatitis (CH) C liver tissues without a history of anti-viral therapy, classified according to the grade of the liver fibrosis (F0, F1, F2, and F3 referred to METAVIR fibrosis stages)(Figure 2, Table S2). Fibrosis grade F0 was considered to be the negative control because these samples were derived from patients with no finding of liver fibrosis. In zebrafish, most highly tissue-specific miRNAs are expressed during embryonic development; approximately 30% of all miRNAs are expressed at a given time point in a given tissue [13]. In mammals, the 20–30% miRNA call rate has recently been validated [14]. Such analysis revealed that the diversity of miRNA expression level among specimens was small. Therefore, we focused on miRNAs with a fold change in mean expression level greater than 1.5 ($p<0.05$) in the two arbitrary groups of liver fibrosis.

Expression of several miRNAs was dramatically different among grades of fibrosis. In the mice study 11 miRNAs were related to the progression of liver fibrosis (mmu-let-7e, miR-125-5p, 199a-5p, 199b, 199b*, 200a, 200b, 31, 34a, 497, and 802). In the human study 10 miRNAs were extracted, and the change in their expression level varied significantly between F0 and F3 (F0<F3: hsa-miR-146b, 199a, 199a*, 200a, 200b, 34a, and 34b, F0>F3: hsa-miR-212, 23b, and 422b). The expression level of 6 miRNAs was significantly different between F0 and F2 (F0<F2: hsa-miR-146b, 200a, 34a, and 34b, F0>F2: hsa-miR-122 and 23b). 5 extracted miRNAs had an expression level that was significantly different between F1 and F2 (F1<F2: hsa-miR-146b, F1>F2: hsa-miR-122, 197, 574, and 768-5p). The expression level of 9 miRNAs changed significantly between F1 and F3 (F1<F3: hsa-miR-146b, 150, 199a, 199a*, 200a, and 200b, F1>F3: hsa-miR-378, 422b, and 768-5p). The miRNAs related to liver fibrosis were extracted using two criteria: similar expression pattern in both the human and the mice specimens and shared sequence between human and mouse. We compared the sequences of mouse miRNAs as described on the Agilent Mouse MiRNA array Version 1.0 (miRbase Version 10.1) and human miRNAs as described on the Agilent Human MiRNA array Version 1.5 (miRbase Version 9.1). The sequences of mmu-miR-199a-5p, mmu-miR-199b, mmu-miR-199b, mmu-miR-200a, and mmu-miR-200b in mouse miRNA corresponded to the sequences of hsa-miR-199a, hsa-miR-199a*, hsa-miR-199a, hsa-miR-200a, and hsa-miR-200b in human miRNA, respectively (Table S3).

Validation of the microarray result by real-time qPCR

The 4 human miRNAs (miR-199a, miR-199a*, miR-200a, and miR-200b) with the largest difference in fold change between the F1 and F3 groups were chosen to validate the microarray results using stem-loop based real-time qPCR. The result of real-time qPCR supported the result of that microarray analysis. The expression level of these 4 miRNAs was significantly different between F0 and F3 and spearman correlation analysis also showed that the expressions of these miRNAs were strongly and positively correlated with fibrosis grade ($n = 105$, $r = 0.498$(miR-199a), 0.607(miR-199a*), 0.639(miR-200a), 0.618(miR-200b), p-values<0.0001) (Figure 3).

Over expression of miR-199a, 199a*, 200a, and 200b was associated with the progression of liver fibrosis

In order to reveal the function of miR-199a, miR-199a*, miR-200a, and miR-200b, we investigated the involvement of these miRNAs in the modulation of fibrosis-related gene in LX-2 cells. The endogenous expression level of these 4 miRNAs in LX2 and normal liver was low according to the microarray study (Figure S2). Transforming growth factor (TGF)β is one of the critical factors for the activation of HSC during chronic inflammation [15] and TGFβ strongly induced expression of three fibrosis-related genes include a matrix degrading complex comprised of α1 procollagen, matrix remodeling complex, comprised of metalloproteinases-13 (MMP-13), tissue inhibitors of metalloproteinases-1 (TIMP-1) in LX-2 cells (Figure 4A). Furthermore, overexpression of miR-199a, miR-199a*, miR-200a and miR-200b in LX-2 cells resulted significant induction of above fibrosis-related genes compared with control miRNA (Figure 4B). Finally we validated the involvement of TGFβ in the modulation of these miRNAs. In LX-2 cells treated with TGFβ, the expression levels of miR-199a and miR-199a* were significantly higher than in untreated cells; the expression levels of miR-200a and miR-200b were significantly lower than in untreated cells. Thus, our in vitro analysis suggested a possible involvement of miR-199a, 199a*, 200a, and 200b in the progression of liver fibrosis.

Discussion

Our comprehensive analysis showed that the aberrant expression of miRNAs was associated with the progression of liver fibrosis. We identified that 4 highly expressed miRNAs (miR-199a, miR-199a*, miR-200a, and miR-200b) that were significantly associated with the progression of liver fibrosis both human and mouse. Coordination of aberrant expression of these miRNAs may contribute to the progression of liver fibrosis.

Prior studies have discussed the expression pattern of miRNA found in liver fibrosis samples between previous and present study. In this report and prior mouse studies and the expression pattern of

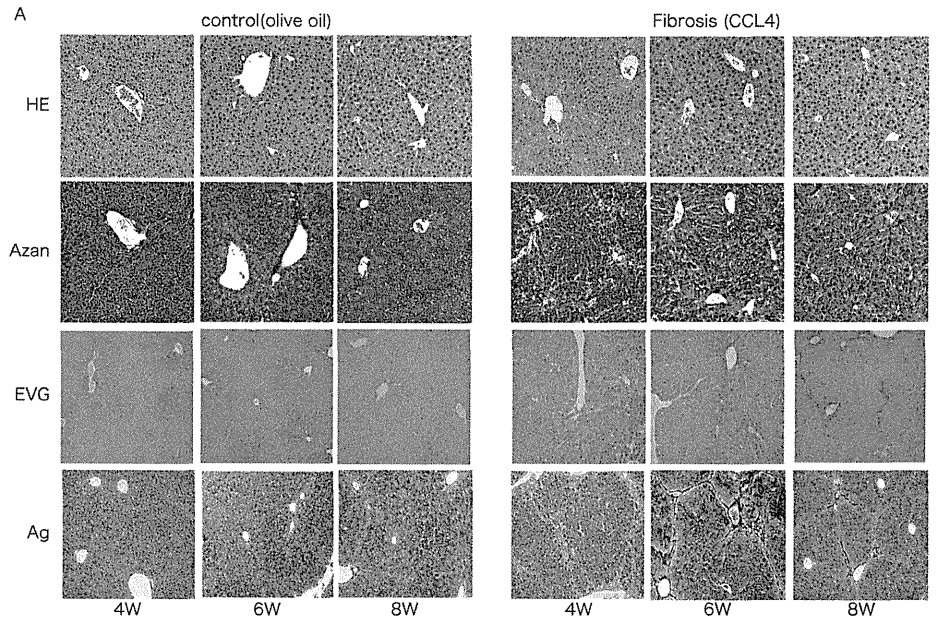

B

miRNA	Fold change CCL4 mouse/control		
	4week	6week	8week
mmu-let-7e	2.92	2.09	2.64
mmu-miR-125a-5p	4.29	2.35	2.67
mmu-miR-199a-5p	2.71	2.12	2.38
mmu-miR-199b	3.25	2.55	2.49
mmu-miR-199b*	5.13	4.47	3.94
mmu-miR-200a	2.23	1.63	2.02
mmu-miR-200b	2.38	2.06	2.20
mmu-miR-31	3.4	2.35	3.19
mmu-miR-34a	3.89	3.22	3.5
mmu-miR-497	2.25	2.00	2.55
mmu-miR-802	2.02	2.87	2.74

Figure 1. The change of liver fibrosis in mouse model. A. Representative H&E-stained, Azan-stained, Ag-stained, and EVG-stained histological sections of liver from mice receiving olive oil alone or CCL_4 in olive oil. Magnification is ×10. B. The expression level of mmu-miRNA in mouse liver with olive oil or CCL_4 at 4W, 6W, and 8W respectively, by microarray analysis.
doi:10.1371/journal.pone.0016081.g001

3 miRNAs (miR-199a-5p, 199b*, 125-5p) was found to be similar while the expression pattern of 11 miRNAs (miR-223, 221, 24, 877, 29b, 29a, 29c, 30c, 365, 148a, and 193) was partially consistent with fibrosis grade [16]. In low graded liver fibrosis, the low expression pattern of 3 miRNAs (miR-140, 27a, and 27b) and the high expression pattern of 6 miRNAs in rat miRNAs (miR-29c*, 143, 872, 193, 122, and 146) in rat miRNA was also similar to our mouse study (GEO Series accession number GSE19865) [11] [12] [17].

The results in this study and previously completed human studies reveal that the expression level of miR-195, 222, 200c, 21, and let-7d was higher in high graded fibrotic liver tissue than in low graded fibrotic liver tissue. Additionally, the expression level of miR-301, 194, and 122 was lower in the high graded fibrotic liver tissue than in low graded fibrotic liver tissue [18] [19] [20](GEO Series accession number GSE16922). This difference in miRNA expression pattern may be contributed to (1) the difference of microarray platform, (2) difference of analytic procedure, and (3) the difference of the species (rat, mouse, and human).

The miR-199 and miR-200 families have are circumstantially related to liver fibrosis. TGFβ-induced factor (TGIF) and SMAD

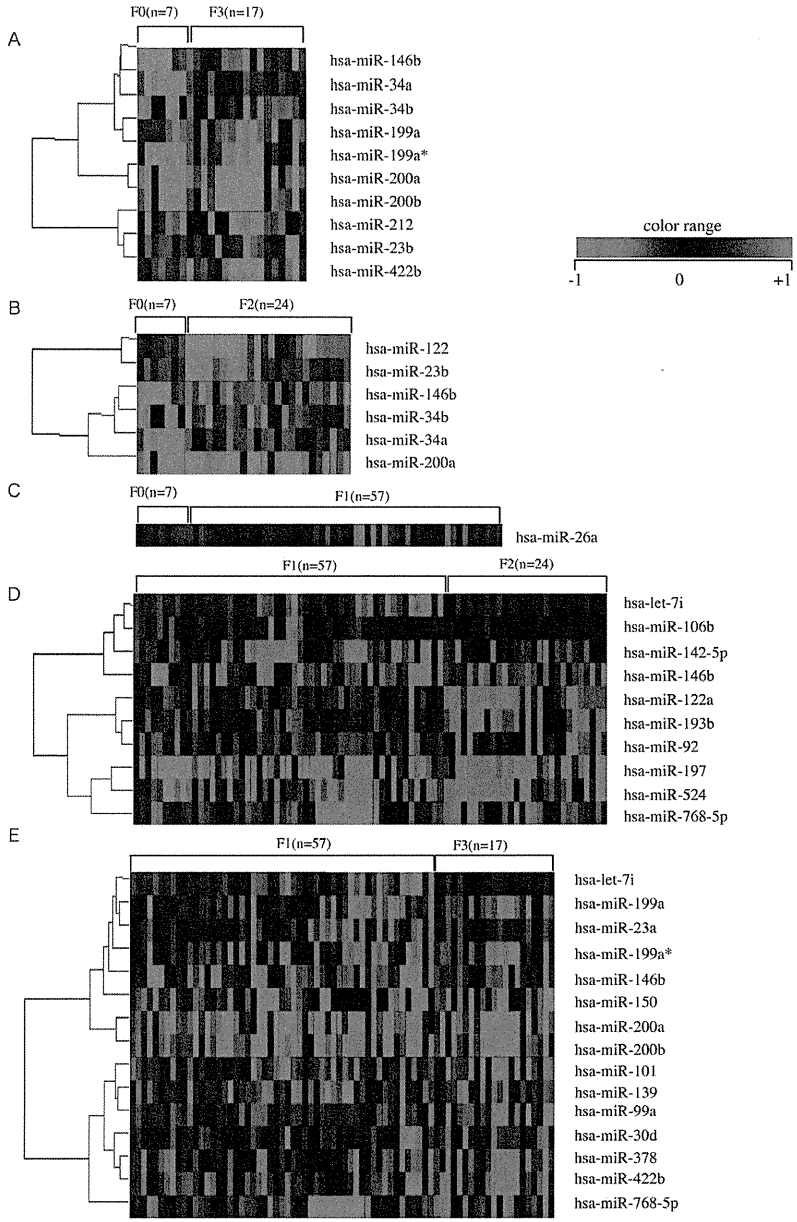

Figure 2. Liver fibrosis in human liver biopsy specimen. A. B. C. D. and E. miRNAs whose expression differs significantly between F0 and F3, F0 and F1, F0 and F2, F1 and F2, and F1 and F3, respectively. Relative expression level of each miRNA in human liver biopsy specimen by microarray. Data from microarray were also statistically analyzed using Welch's test and the Bonferroni correction for multiple hypotheses testing. Fold change, p-value are listed in Table S2.
doi:10.1371/journal.pone.0016081.g002

specific E3 ubiquitin protein ligase 2 (SMURF2), both of which play roles in the TGFβ signaling pathway, are candidate targets of miR-199a* and miR-200b, respectively, as determined by the Targetscan algorithm. The expression of miR-199a* was silenced in several proliferating cell lines excluding fibroblasts [21]. Down regulation of miR-199a, miR-199a* and 200a in chronic liver injury tissue was associated with the hepatocarcinogenesis [9]. miR-199a* is also one of the negative regulators of the HCV replication [22]. According to three target search algorithms (Pictar, miRanda, and Targetscan), the miRNAs that may be associated with the liver fibrosis can regulate several fibrosis-related genes (Table S4). Aberrant expression of these miRNAs may be closely related to the progress of the chronic liver disease.

Epithelial-mesenchymal transition (EMT) describes a reversible series of events during which an epithelial cell loses cell-cell contacts and acquires mesenchymal characteristics [23]. Although EMT is not a common event in adults, this process has been implicated in such instances as wound healing and fibrosis. Recent reports showed that the miR-200 family regulated EMT by targeting EMT accelerator ZEB1 and SIP1 [24]. From our observations, overexpression of miR-200a and miR-200b can be connected to the progression of liver fibrosis.

The diagnosis and quantification of fibrosis have traditionally relied on liver biopsy, and this is still true at present. However, there are a number of drawbacks to biopsy, including the invasive nature of the procedure and inter-observer variability. A number of staging systems have been developed to reduce both the inter-observer variability and intra-observer variability, including the METAVIR, the Knodell fibrosis score, and the Scheuer score. However, the reproducibility of hepatic fibrosis and inflammatory activity is not as consistent [25]. In fact, in our study, the degree of fibrosis of the two arbitrary fibrosis groups was classified using the miRNA expression profile with 80% or greater accuracy (data not shown). Thus, miRNA expression can be used for diagnosis of liver fibrosis.

In this study we investigated whether common miRNAs in human and mouse could influence the progression of the liver fibrosis. The signature of miRNAs expression can also serves as a tool for understanding and investigating the mechanism of the onset and progression of liver fibrosis. The miRNA expression profile has the potential to be a novel biomarker of liver fibrosis.

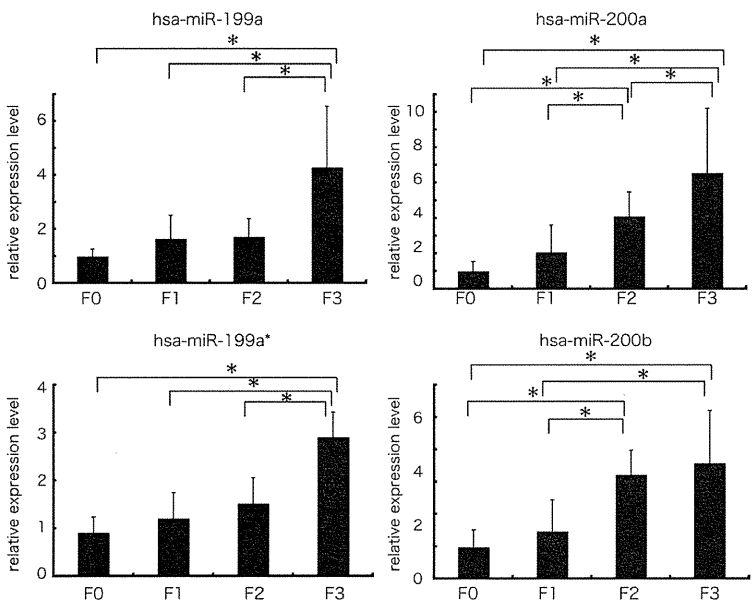

Figure 3. The expression level of miR-199 and 200 families in human liver biopsy specimen by real-time qPCR. Real-time qPCR validation of the 4 miRNAs (miR-199a, miR-199a*, miR-200a, and miR-200b). Each column represents the relative amount of miRNAs normalized to the expression level of U18. The data shown are the means+SD of three independent experiments. Asterisks indicates to a significant difference of $p<0.05$ (two-tailed Student-t test), respectively.
doi:10.1371/journal.pone.0016081.g003

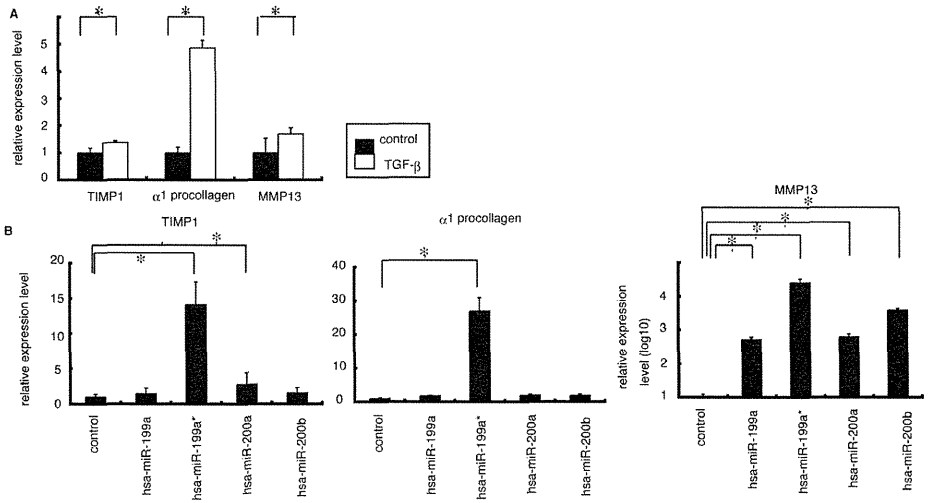

Figure 4. The relationship between expression level of miR-199 and 200 families and expression level of three fibrosis related genes. A. Administration of TGFβ in LX2 cells showed that the expression level of three fibrosis related genes were higher than that in non-treated cells. The data shown are the means+SD of three independent experiments. Asterisk was indicated to the significant difference of $p<0.05$ (two-tailed Student-t test). B. The expression levels of 3 fibrosis related genes in LX2 cells with overexpressing miR-199a, 199a*, 200a, or 200b, respectively were significantly higher than that in cells transfected with control miRNA ($p<0.05$; two-tailed Student t-test).
doi:10.1371/journal.pone.0016081.g004

Moreover miRNA expression profiling has further applications in novel anti-fibrosis therapy in CH.

Materials and Methods

Sample preparation

105 liver tissues samples from chronic hepatitis C patients (genotype 1b) were obtained by fine needle biopsy (Table S1). METAVIR fibrosis stages were F0 in 7 patients, F1 in 57, F2 in 24 and F3 in 17. Patients with autoimmune hepatitis or alcoholic liver injury were excluded. None of the patients were positive for hepatitis B virus associated antigen/ antibody or anti human immunodeficiency virus antibody. No patient received interferon therapy or immunomodulatory therapy prior to the enrollment in this study. We also obtained normal liver tissue from the Liver Transplantation Unit of Kyoto University. All of the patients or their guardians provided written informed consent, and Kyoto University Graduate School and Faculty of Medicine's Ethics Committee approved all aspects of this study in accordance with the Helsinki Declaration.

RNA preparation and miRNA microarray

Total RNA from cell lines or tissue samples was prepared using a *mir*Vana miRNA extraction Kit (Ambion, Austin, TX, USA) according to the manufacturer's instruction. miRNA microarrays were manufactured by Agilent Technologies (Santa Clara, CA, USA) and 100 ng of total RNA was labeled and hybridized using the Human microRNA Microarray Kit protocol for use with Agilent microRNA microarrays Version 1.5 and Mouse microRNA Microarray Kit protocol for use with Agilent microRNA microarrays Version 1.0. Hybridization signals were detected with a DNA microarray scanner G2505B (Agilent Technologies) and the scanned images were analyzed using Agilent feature extraction software (v9.5.3.1). Data were analyzed using GeneSpring GX 7.3.1 software (Agilent Technologies) and normalized as follows: (i) Values below 0.01 were set to 0.01. (ii) In order to compare between one-color expression profile, each measurement was divided by the 75th percentile of all measurements from the same species. The data presented in this manuscript have been deposited in NCBI's Gene Expression Omnibus and are accessible through GEO Series accession number GSE16922 (human) and accession number GSE19865 (mouse).

Real-time qPCR for human miRNA

For detection of the miRNA level by real-time qPCR, TaqMan® microRNA assay (Applied Biosystems) was used to quantify the relative expression level of miR-199a (assay ID. 002304), miR-199a* (assay ID. 000499), miR-200a (assay ID. 000502), miR-200b (assay ID. 002251), and U18 (assay ID. 001204) was used as an internal control. cDNA was synthesized using the Taqman miRNA RT Kit (Applied Biosystems). Total RNA (10 ng/ml) in 5ml of nuclease free water was added to 3 ml of 5× RT primer, 10× 1.5μl of reverse transcriptase buffer, 0.15 μl of 100 mM dNTP, 0.19 μl of RNase inhibitor, 4.16 μl of nuclease free water, and 50U of reverse transcriptase in a total volume of 15 μl. The reaction was performed for 30 min at 16°C, 30 min at 42°C, and 5 min at 85°C. All reactions were run in triplicate. Chromo 4 detector (BIO-RAD) was used to detect miRNA expression.

Animal and Chronic Mouse Liver Injury Model

Each 5 adult (8-week-old) male C57BL/6J mice were given a biweekly intra-peritoneal dose of a 10% solution of CCl_4 in olive oil (0.02 ml/g/ mouse) for the first 4 weeks and then once a week for the next 4 weeks. At week 4, 6 or 8, the mice were sacrificed. Partial livers were fixed, embedded in paraffin, and processed for histology. Serial liver sections were stained with hematoxylin-eosin, Azan staining, Silver (Ag) staining, and Elastica van Gieson (EVG) staining, respectively. Total RNA from mice liver tissue was prepared as described previously. All animal procedures concerning the analysis of liver injury were performed in following the guidelines of the Kyoto University Animal Research Committee and were approved by the Ethical Committee of the Faculty of Medicine, Kyoto University.

Cell lines and Cell preparation

The human stellate cell lines LX-2, was provided by Scott L. Friedman. LX-2 cells, which viable in serum free media and have high transfectability, were established from human HSC lines [26]. LX-2 cells were maintained in D-MEM (Invitrogen, Carlsbad, CA, USA) with 10% fetal bovine serum, plated in 60 mm diameter dishes and cultured to 70% confluence. Huh-7 and Hela cells were also maintained in D-MEM with 10% fetal bovine serum. HuS-E/2 immortalized hepatocytes were cultured as described previously [27]. LX-2 cells were then cultured in D-MEM without serum with 0.2% BSA for 48 hours prior to TGFβ1 (Sigma-Aldrich, Suffolk, UK) treatment (2.5 ng/ml for 20 hours). Control cells were cultured in D-MEM without fetal bovine serum.

miRNA transfection

LX-2 cells were plated in 6-well plates the day before transfection and grown to 70% confluence. Cells were transfected with 50 pmol of Silencer® negative control siRNA (Ambion) or double-stranded mature miRNA (Hokkaido System Science, Sapporo, Japan) using lipofectamine RNAiMAX (Invitrogen). Cells were harvested 2 days after transfection.

Real-time qPCR

cDNA was synthesized using the Transcriptor High Fidelity cDNA synthesis Kit (Roche, Basel, Switzerland). Total RNA (2 μg) in 10.4 μl of nuclease free water was added to 1 μl of 50mM random hexamer. The denaturing reaction was performed for 10min at 65°C. The denatured RNA mixture was added to 4 μl of 5× reverse transcriptase buffer, 2 μl of 10 mM dNTP, 0.5 μl of 40U/μl RNase inhibitor, and 1.1 μl of reverse transcriptase (FastStart Universal SYBR Green Master (Roche) in a total volume of 20 μl. The reaction ran for 30 min at 50°C (cDNA synthesis), and five min at 85°C (enzyme denaturation). All reactions were run in triplicate. Chromo 4 detector (BIO-RAD, Hercules, CA, USA) was used to detect mRNA expression. The primer sequences are follows; MMP13 s; 5′-gaggctccgagaaatgcagt-3′, as; 5′-atgccatcgtgaagtctggt-3′, TIMP1 s; 5′-cttggcttctgcactgatgg-3′, as; 5′-acgctggtataaggtggtct-3′, α1-procollagen s; 5′-aacatgaccaaaaaccaaaagtg-3′, as; 5′-catt-gtttcctgtgtcttctgg-3′, and β-actin s; 5′-ccactggcatcgtgatggac-3′, as; 5′-tcattgccaatggtgatgacct-3′. Assays were performed in triplicate, and the expression levels of target genes were normalized to expression of the β-actin gene, as quantified using real-time qPCR as internal controls.

Statistical analyses

Statistical analyses were performed using Student's *t*-test; *p* values less than 0.05 were considered statistically significant. Microarray data were also statistically analyzed using Welch's test and Bonferroni correction for multiple hypotheses testing.

Supporting Information

Figure S1 Time line of the induction of chronic liver fibrosis. Upward arrow indicated administration of olive oil or CCl_4. Downward arrow indicates when mice were sacrificed.
(TIF)

Figure S2 Comparison of the expression level of miR-199 and 200 familes in several cell lines and human liver tissue. Endogenous expression level of miR-199a, 199a*, 200a, and 200b in normal liver and LX2 cell as determined by microarray analysis (Agilent Technologies). Endogenous expression level of same miRNAs in Hela, Huh-7 and, immortalized hepatocyte: HuS-E/2 by previously analyzed data [9].
(TIF)

Table S1 Clinical characteristics of patients by the grade of fibrosis.
(DOCX)

Table S2 Extracted human miRNAs related to liver fibrosis.
(DOCX)

Table S3 Corresponding human and mouse miRNAs.
(DOCX)

Table S4 Hypothetical miRNA target genes according to in silico analysis.
(DOCX)

Author Contributions

Conceived and designed the experiments: YM KS. Performed the experiments: YM HT YH NK. Analyzed the data: MT MK. Contributed reagents/materials/analysis tools: YM HT YH NK. Wrote the paper: YM MT AT FM NK TO.

References

1. Wasley A, Alter MJ (2000) Epidemiology of hepatitis C: geographic differences and temporal trends. Semin Liver Dis 20: 1–16.
2. Shepard CW, Finelli L, Alter MJ (2005) Global epidemiology of hepatitis C virus infection. Lancet Infect Dis 5: 558–567.
3. Gressner AM, Weiskirchen R (2006) Modern pathogenetic concepts of liver fibrosis suggest stellate cells and TGF-beta as major players and therapeutic targets. J Cell Mol Med 10: 76–99.
4. Nilsen TW (2007) Mechanisms of microRNA-mediated gene regulation in animal cells. Trends Genet 23: 243–249.
5. Zamore PD, Haley B (2005) Ribo-gnome: the big world of small RNAs. Science 309: 1519–1524.
6. Pillai RS (2005) MicroRNA function: multiple mechanisms for a tiny RNA? Rna 11: 1753–1761.
7. Ura S, Honda M, Yamashita T, Ueda T, Takatori H, et al. (2009) Differential microRNA expression between hepatitis B and hepatitis C leading disease progression to hepatocellular carcinoma. Hepatology 49: 1098–1112.
8. Yamamoto Y, Kosaka N, Tanaka M, Koizumi F, Kanai Y, et al. (2009) MicroRNA-500 as a potential diagnostic marker for hepatocellular carcinoma. Biomarkers 14: 529–538.
9. Murakami Y, Yasuda T, Saigo K, Urashima T, Toyoda H, et al. (2006) Comprehensive analysis of microRNA expression patterns in hepatocellular carcinoma and non-tumorous tissues. Oncogene 25: 2537–2545.
10. Jin X, Ye YF, Chen SH, Yu CH, Liu J, et al. (2008) MicroRNA expression pattern in different stages of nonalcoholic fatty liver disease. Dig Liver Dis.
11. Ogawa T, Iizuka M, Sekiya Y, Yoshizato K, Ikeda K, et al. (2009) Suppression of type I collagen production by microRNA-29b in cultured human stellate cells. Biochem Biophys Res Commun.
12. Ji J, Zhang J, Huang G, Qian J, Wang X, et al. (2009) Over-expressed microRNA-27a and 27b influence fat accumulation and cell proliferation during rat hepatic stellate cell activation. FEBS Lett 583: 759–766.
13. Wienholds E, Kloosterman WP, Miska E, Alvarez-Saavedra E, Berezikov E, et al. (2005) MicroRNA expression in zebrafish embryonic development. Science 309: 310–311.

14. Landgraf P, Rusu M, Sheridan R, Sewer A, Iovino N, et al. (2007) A mammalian microRNA expression atlas based on small RNA library sequencing. Cell 129: 1401–1414.
15. Friedman SL (2008) Hepatic fibrosis-Overview. Toxicology.
16. Roderburg C, Urban GW, Bettermann K, Vucur M, Zimmermann H, et al. (2010) Micro-RNA profiling reveals a role for miR-29 in human and murine liver fibrosis. Hepatology.
17. Venugopal SK, Jiang J, Kim TH, Li Y, Wang SS, et al. (2010) Liver fibrosis causes downregulation of miRNA-150 and miRNA-194 in hepatic stellate cells, and their overexpression causes decreased stellate cell activation. Am J Physiol Gastrointest Liver Physiol 298: G101–106.
18. Jiang J, Gusev Y, Aderca I, Mettler TA, Nagorney DM, et al. (2008) Association of MicroRNA expression in hepatocellular carcinomas with hepatitis infection, cirrhosis, and patient survival. Clin Cancer Res 14: 419–427.
19. Jiang X, Tsitsiou E, Herrick SE, Lindsay MA (2010) MicroRNAs and the regulation of fibrosis. Febs J 277: 2015–2021.
20. Marquez RT, Bandyopadhyay S, Wendlandt EB, Keck K, Hoffer BA, et al. (2010) Correlation between microRNA expression levels and clinical parameters associated with chronic hepatitis C viral infection in humans. Lab Invest.
21. Kim S, Lee UJ, Kim MN, Lee EJ, Kim JY, et al. (2008) MicroRNA miR-199a* regulates the MET proto-oncogene and the downstream extracellular signal-regulated kinase 2 (ERK2). J Biol Chem 283: 18158–18166.
22. Murakami Y, Aly HH, Tajima A, Inoue I, Shimotohno K (2009) Regulation of the hepatitis C virus genome replication by miR-199a. J Hepatol 50: 453–460.
23. Gibbons DL, Lin W, Creighton CJ, Rizvi ZH, Gregory PA, et al. (2009) Contextual extracellular cues promote tumor cell EMT and metastasis by regulating miR-200 family expression. Genes Dev 23: 2140–2151.
24. Gregory PA, Bert AG, Paterson EL, Barry SC, Tsykin A, et al. (2008) The miR-200 family and miR-205 regulate epithelial to mesenchymal transition by targeting ZEB1 and SIP1. Nat Cell Biol 10: 593–601.
25. Oberti F, Valsesia E, Pilette C, Rousselet MC, Bedossa P, et al. (1997) Noninvasive diagnosis of hepatic fibrosis or cirrhosis. Gastroenterology 113: 1609–1616.
26. Xu L, Hui AY, Albanis E, Arthur MJ, O'Byrne SM, et al. (2005) Human hepatic stellate cell lines, LX-1 and LX-2: new tools for analysis of hepatic fibrosis. Gut 54: 142–151.
27. Aly HH, Watashi K, Hijikata M, Kaneko H, Takada Y, et al. (2007) Serum-derived hepatitis C virus infectivity in interferon regulatory factor-7-suppressed human primary hepatocytes. J Hepatol 46: 26–36.

Available online at www.sciencedirect.com
ScienceDirect
Current Opinion in Immunology
ELSEVIER

Helicobacter pylori-induced activation-induced cytidine deaminase expression and carcinogenesis

Hiroyuki Marusawa and Tsutomu Chiba

Tumorigenesis is a multistep process in which the accumulation of genetic alterations drives the transformation of normal cells into malignant derivatives. Activation-induced cytidine deaminase (AID) contributes to immune system diversity by inducing somatic hypermutations and class-switch recombinations of human immunoglobulin genes. The mutagenic activity of AID, however, can also induce genetic changes in various genes and may lead to the development of cancer. *Helicobacter pylori*, a class 1 carcinogen for human gastric cancer, affects AID expression by two different mechanisms, introduction of bacterial virulence factors into host cells and induction of inflammatory responses, thereby contributing to the accumulation of mutations in tumor-related genes. Aberrant AID activity may therefore be a novel link between infection and carcinogenesis.

Address
Department of Gastroenterology and Hepatology, Graduate School of Medicine, Kyoto University, 54 Kawara-cho, Shogoin, Sakyo-ku, Kyoto 606-8507, Japan

Corresponding author: Marusawa, Hiroyuki (maru@kuhp.kyoto-u.ac.jp)

Current Opinion in Immunology 2010, **22**:442–447

This review comes from a themed issue on
Host pathogens
Edited by Adolfo Garcia-Sastre and Philippe Sansonetti

0952-7915/$ – see front matter

DOI 10.1016/j.coi.2010.06.001

Introduction

Helicobacter pylori (*H. pylori*) is a gram-negative, spiral-shaped bacterium colonized in human populations for more than 58,000 years [1]. *H. pylori* infection is involved in the development of several human diseases, including gastro-duodenal ulcers, gastric cancer, and mucosa-associated lymphoid tissue (MALT) lymphoma of the stomach. *H. pylori* strains exhibit a high level of genetic diversity, and a striking difference among strains is the presence or absence of a 40-kb DNA segment, termed the cag pathogenicity island (PAI). The risk for developing *H. pylori* infection-mediated gastric disorders is closely associated with the strain [2]. The risk of developing gastric cancer is higher in patients infected with cagPAI-positive *H. pylori* compared with cagPAI-negative *H. pylori* [3,4], but how *H. pylori* infection contributes to gastric carcinogenesis remained unknown. Genetic changes in tumor-related genes are essential in the malignant transformation that leads to cancer cell development. How the intra-gastric residential bacteria induce the genetic changes required for tumorigenesis in host gastric epithelial cells is unclear, since the extracellular habitant *H. pylori* cannot directly access host genomic DNA located in the nucleus of gastric epithelial cells. Recent studies, however, revealed that cagPAI-positive *H. pylori* manipulates the host nucleotide editing enzymes to induce mutagenesis in human DNA sequences of the gastric epithelium [5].

Novel mechanism of active mutagenesis achieved by nucleotide editing enzymes

Genetic changes in tumor-related genes are essential for malignant transformation in cancer cell development. Mechanisms that account for genetic changes required for tumorigenesis are unknown, except for defects in the DNA repair system that are observed in certain human cancers. Several enzymes that induce nucleotide alterations were recently identified, providing a new avenue for understanding the mutagenesis mechanism. The apolipoprotein B mRNA editing enzyme catalytic polypeptide (APOBEC) family comprises nucleotide editing enzymes that insert nucleotide alterations in target DNA or RNA through cytidine deamination [6]. The human APOBEC family consists of APOBEC1, APOBEC2, APOBEC3A, APOBEC3B, APOBEC3C, APOBEC3DE, APOBEC3F, APOBEC3G, APOBEC3H, APOBEC4, and activation-induced cytidine deaminase (AID), and contributes to producing various favorable physiologic outcomes by modifying target gene sequences. For example, APOBEC1 participates in lipid metabolism through deaminating a specific cytidine to uridine in the Apo-B mRNA, resulting in the formation of a termination codon, which leads to the production of a half-length genomically encoded Apo-B100. APOBEC3G is an anti-viral molecule that induces hypermutation in viral DNA sequences and acts as a host defense factor against viruses such as HIV-1. Although the majority of APOBEC family members exhibit mutagenic activity against human RNA or exogenous viral genomes, only AID has the ability to induce nucleotide alterations and double-strand DNA breaks in human genomic sequences. Under physiologic conditions, AID is expressed in germinal center B cells and induces somatic hypermutation and class-switch recombination of immunoglobulin genes, thereby amplifying immune system diversity [7]. In sharp contrast to the favorable role of AID in the immune system, excessive AID activity might affect non-immunoglobulin

genes, including tumor-related genes in non-lymphoid cells [8].

CagPAI-positive *H. pylori* induces aberrant AID expression in gastric epithelial cells

AID can alter host genomic information, but there are safeguard mechanisms that restrict its potential tumorigenic activity, including post-transcriptional regulation by microRNA [9,10,11•], post-translational modification by protein phosphorylation or ubuiquitination [12–14], and regulation of subcellular localization [15–18]. Restriction of AID expression is also an important regulatory system that minimizes the aberrant mutagenic activity of AID. AID gene transcription is restricted mainly to activated germinal center B lymphocytes where editing of the immunoglobulin gene is required [19,20], while AID expression is not detected in normal epithelial cells under physiologic conditions. How then is AID expressed in epithelial cells under pathologic conditions, especially where the tumorigenic risk is unusually high? Strikingly, endogenous AID is expressed in the epithelial cells of *H. pylori*-infected stomach. Gastric epithelial cells and some infiltrating lymphocytes are immunoreactive for AID protein expression in the majority of chronic gastritis tissues infected with cagPAI-positive *H. pylori* [21]. Moreover, eradication of *H. pylori* infection by antibiotics substantially decreases AID protein expression in gastric mucosa. These findings suggest that cagPAI-positive *H. pylori* somehow upregulates AID protein in the gastric epithelium of the infected host.

CagPAI contain approximately 30 putative genes encoding various bacterial proteins such as cytotoxin-associated gene A (cagA) [22]. CagPAI-positive *H. pylori* introduces several bacterial virulence factors into gastric epithelial cells through a type-IV secretion apparatus, and cagPAI-positive *H. pylori*-derived peptidoglycans introduced into the host cells have been shown to be responsible for activating the transcription factor NF-κB [23]. The AID promoter region also includes sites for several transcription factors, such as NF-κB, STAT6, HoxC4, Sp1, Sp3, and Pax5 [24–27], and AID expression in B lymphocytes is induced in response to NF-κB activation through CD40 ligand signaling [28]. Together, these findings suggest that cagPAI-positive *H. pylori* induces AID expression via NF-κB activation by introducing bacterial virulence factors, and that the proinflammatory response caused by *H. pylori* infection also triggers AID expression via the activation of NF-κB in gastric epithelium, because proinflammatory cytokines such as tumor necrosis factor

Figure 1

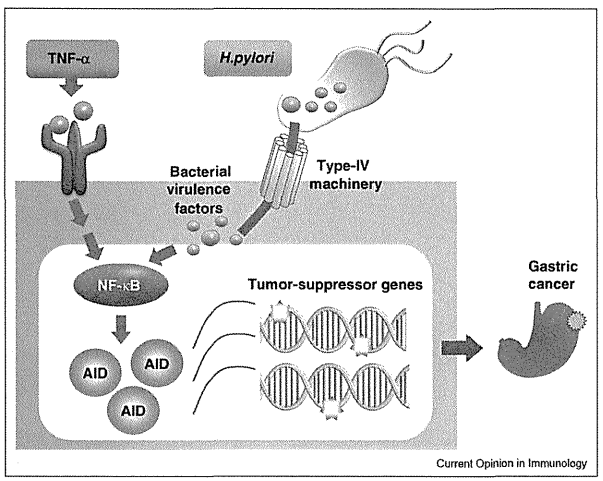

Helicobacter pylori infection triggers AID expression in gastric epithelial cells via two distinct pathways. AID acts as a cytidine deaminase that is capable of inducing nucleotide alterations in human DNA sequences. Under physiologic conditions, no AID expression is detectable in normal gastric epithelium. *Helicobacter pylori* (*H. pylori*) infection, however, can induce AID expression in gastric epithelial cells via two distinct pathways. CagPAI-positive *H. pylori* strains possess type-IV machinery and can inject bacterial virulence factors into gastric epithelial cells, leading to the activation of the host transcriptional factor NF-κB. The host inflammatory response triggered by *H. pylori* infection also activates NF-κB in gastric epithelium. As a result, AID is transcriptionally upregulated in gastric epithelial cells, and can contribute to the production of unfavorable genetic changes in tumor-related genes, leading to gastric carcinogenesis.

Author's personal copy

(TNF)-α and IL-1β can induce NF-κB activation in various types of cells. These hypotheses are supported by *in vitro* analyses showing that AID expression is induced in response to cagPAI-positive *H. pylori* infection or stimulation with the proinflammatory cytokine TNF-α via NF-κB signaling in cultured human gastric epithelial cells [21]. Based on the clinical course of *H. pylori*-infected individuals, both bacterial factors that are introduced into epithelial cells and the inflammatory response against *H. pylori* infection would be responsible for aberrant AID expression in gastric epithelium (Figure 1), and the direct action of the bacterial virulence factors contributes to activate AID in the early stage of *H. pylori* infection when the number of bacteria is high. In the late phase of chronic gastritis, when gastric atrophy has progressed and the number of *H. pylori* is decreased, the proinflammatory cytokine plays a central role in causing the constitutive expression of AID in gastric epithelial cells.

AID induces DNA mutations in tumor-related genes in gastric epithelial cells

The target of AID-mediated genotoxic effects is not restricted to immunoglobulin genes and several non-immunoglobulin genes are also targeted by AID in lymphocytes. Approximately 25% of expressed non-immunoglobulin genes analyzed, including Bcl6 and Cd83, accumulated AID-mediated mutations in germinal B cells [29••]. Moreover, AID produces double-strand DNA breaks throughout the genome, including *c-myc* in B cells [30,31•]. The impact of AID expression in non-lymphoid gastrointestinal epithelial cells was clarified using mouse model with constitutive and ubiquitous AID expression. AID transgenic mice accumulated somatic mutations in various tumor-related genes and developed tumors in both lymphoid and non-lymphoid tissues [32,33]. The tumors developed in the epithelial organs of AID transgenic mice included lung, liver, and gastric cancers.

The findings that AID mutagenic activity results in stomach cancer led us to speculate that *H. pylori* infection in association with aberrant AID expression contributes to human carcinogenesis via the accumulation of genetic alterations in gastric epithelial cells [21]. In *in vitro*-cultured gastric epithelial cells, cagPAI-positive *H. pylori* infection led to somatic mutations in the tumor-suppressor *TP53* gene. The number of nucleotide alterations observed in *H. pylori*-infected cells was significantly reduced by knockdown of

Figure 2

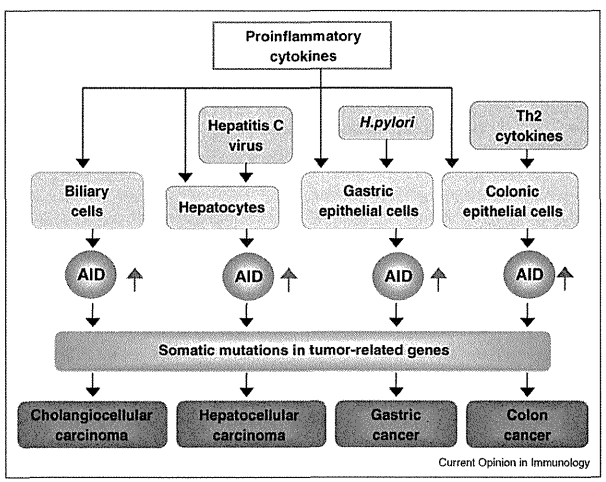

AID links inflammation and infection to cancer development in various gastrointestinal tissues. This figure is a model depicting the role of AID in the development of human cancers. Normal epithelial cells lack endogenous AID expression under physiologic conditions. *Helicobacter pylori* (*H. pylori*) infection and the resultant inflammatory stimulation, however, trigger aberrant AID expression in gastric epithelial cells. Similarly, hepatitis C virus infection and the resultant constitutive inflammation lead to AID expression in hepatocytes. In addition to proinflammatory cytokines, Th2 cytokine plays a role in the enhanced expression of AID in colonic epithelium. Constitutive AID activation in these epithelial cells results in the accumulation of somatic mutations in various target genes. If crucial nucleotide changes in the tumor-related genes are induced by AID activity, the resultant cells can acquire the transformation, leading to cancer development.

endogenous AID, indicating that the somatic mutations in the *TP53* gene in cells infected with cagPAI-positive *H. pylori* were due to the induction of endogenous AID expression in gastric cells. In wild-type mice, oral infection with cagPAI-positive *H. pylori* upregulated AID protein expression. Moreover, nucleotide alterations emerge in the *TP53* gene in stomach tissues after oral *H. pylori* infection in wild-type mice. These findings strongly suggest that *H. pylori* infection causes accumulation of somatic mutations in tumor-related genes such as *TP53* through aberrant upregulation of AID in gastric epithelial cells.

H. pylori-associated lymphoid tumorigenesis and AID expression

Low-grade lymphomas originating from MALT develop in the stomach, salivary and thyroid glands, bronchi, and small intestine, and are classified as MALT lymphoma [34,35]. The acquisition of MALT is induced before the development of lymphoma as a response to a persistent antigenic stimulation [36]. The development of gastric MALT lymphoma, a representative gastric lymphoma, is strongly associated with *H. pylori* infection [37]. The seroprevalence of *H. pylori* is higher in patients with gastric MALT lymphomas than in control patients without MALT lymphoma [38], and eradication of *H. pylori* leads to complete regression of the lymphoma in nearly 80% of patients with early-stage disease [39,40]. On the contrary, several studies have aimed to clarify the role of AID in the development of MALT lymphoma, because AID is required for the development of germinal center-derived non-Hodgkin's lymphomas [41,42•]. AID mRNA was, however, expressed in only some extranodal marginal zone B-cell MALT lymphomas [41]. More recent studies demonstrate that neoplastic marginal zone B cells did not express detectable AID, whereas AID expression was confined to reactive areas within MALT lymphomas [43,44]. In addition to the low frequency of AID upregulation in MALT lymphoma tissues, it remains unknown whether *H. pylori* infection enhances the aberrant mutagenic activity of AID in gastric B cells. Further analyses are required to determine the role of AID in the development of *H. pylori*-associated MALT lymphomas.

Conclusions

The discovery of AID was a seminal finding that greatly advanced our understanding of the molecular mechanisms involved in immunoglobulin diversification [45]. Now, AID is central to our understanding of how inflammation and infection underlie the genetic alterations required for carcinogenesis in epithelial cells [46]. Indeed, proinflammatory cytokine induction of AID expression via the NF-κB pathway is not limited to gastric epithelial cells. AID expression is mediated by the inflammatory response in a variety of epithelial cells, including human hepatocytes [47,48••], and biliary [49] and colonic epithelial cells [50•]. Aberrant AID expression in these gastrointestinal organs results in somatic mutations in various tumor-related genes. Thus, AID may have a central role in genetic susceptibility to mutagenesis, which leads to cancers in these gastrointestinal tissues upon exposure to certain inflammation or infection (Figure 2).

A characteristic of *H. pylori*-associated gastric cancer is multicentric tumor development. Patients with a history of *H. pylori*-related gastric cancer are at high risk for subsequent development of gastric cancers [51], suggesting that each epithelial cell of the *H. pylori*-infected stomach possesses sufficient genetic damage for malignant transformation. Efficient strategies to restrict aberrant AID activity might help to prevent carcinogenesis in gastric epithelial cells inflamed by *H. pylori* infection.

Acknowledgements

We are grateful to K. Kinoshita for his useful suggestions and critical reading of our manuscript. HM is supported by the grant from the Ministry of Education, Culture, Sports, Science, and Research Grant of the Princess Takamatsu Cancer Research and Takeda Research Fund.

Conflict of interest

None.

References and recommended reading

Papers of particular interest, published within the annual period of review, have been highlighted as:

- • of special interest
- •• of outstanding interest

1. Linz B, Balloux F, Moodley Y, Manica A, Liu H, Roumagnac P, Falush D, Stamer C, Prugnolle F, van der Merwe SW *et al.*: **An African origin for the intimate association between humans and *Helicobacter pylori***. *Nature* 2007, **445**:915-918.

2. Cover TL, Blaser MJ: ***Helicobacter pylori* in health and disease**. *Gastroenterology* 2009, **136**:1863-1873.

3. Huang JQ, Zheng GF, Sumanac K, Irvine EJ, Hunt RH: **Meta-analysis of the relationship between cagA seropositivity and gastric cancer**. *Gastroenterology* 2003, **125**:1636-1644.

4. Basso D, Zambon CF, Letley DP, Stranges A, Marchet A, Rhead JL, Schiavon S, Guariso G, Ceroti M, Nitti D *et al.*: **Clinical relevance of *Helicobacter pylori* cagA and vacA gene polymorphisms**. *Gastroenterology* 2008, **135**:91-99.

5. Chiba T, Marusawa H: **A novel mechanism for inflammation-associated carcinogenesis; an important role of activation-induced cytidine deaminase (AID) in mutation induction**. *J Mol Med* 2009, **87**:1023-1027.

6. Conticello SG: **The AID/APOBEC family of nucleic acid mutators**. *Genome Biol* 2008, **9**:229.

7. Shivarov V, Shinkura R, Doi T, Begum NA, Nagaoka H, Okazaki IM, Ito S, Nonaka T, Kinoshita K, Honjo T: **Molecular mechanism for generation of antibody memory**. *Philos Trans R Soc Lond B Biol Sci* 2009, **364**:569-575.

8. Kinoshita K, Nonaka T: **The dark side of activation-induced cytidine deaminase: relationship with leukemia and beyond**. *Int J Hematol* 2006, **83**:201-207.

9. Dorsett Y, McBride KM, Jankovic M, Gazumyan A, Thai TH, Robbiani DF, Di Virgilio M, San-Martin BR, Heidkamp G, Schwickert TA *et al.*: **MicroRNA-155 suppresses activation-induced cytidine deaminase-mediated Myc-Igh translocation**. *Immunity* 2008, **28**:630-638.

10. Teng G, Hakimpour P, Landgraf P, Rice A, Tuschl T, Casellas R, Papavasiliou FN: **MicroRNA-155 is a negative regulator of activation-induced cytidine deaminase**. *Immunity* 2008, **28**:621-629.

11. • de Yebenes VG, Belver L, Pisano DG, Gonzalez S, Villasante A, Croce C, He L, Ramiro AR: **miR-181b negatively regulates activation-induced cytidine deaminase in B cells**. *J Exp Med* 2008, **205**:2199-2206.
References [9] and [10] demonstrate that microRNA-155 (miR-155) is upregulated in B lymphocytes undergoing class-switch recombination and regulate the transcription of AID by targeting the 3′ untranslated region of the AID mRNA, suggesting the possible role of miR-155 as a tumor suppressor by inhibiting the genotoxic effect of AID. Similarly, reference 11 showed the negative regulation of AID transcription by another microRNA-181b.

12. McBride KM, Gazumyan A, Woo EM, Schwickert TA, Chait BT, Nussenzweig MC: **Regulation of class switch recombination and somatic mutation by AID phosphorylation**. *J Exp Med* 2008, **205**:2585-2594.

13. Cheng HL, Vuong BQ, Basu U, Franklin A, Schwer B, Astarita J, Phan RT, Datta A, Manis J, Alt FW *et al.*: **Integrity of the AID serine-38 phosphorylation site is critical for class switch recombination and somatic hypermutation in mice**. *Proc Natl Acad Sci USA* 2009, **106**:2717-2722.

14. Aoufouchi S, Faili A, Zober C, D'Orlando O, Weller S, Weill JC, Reynaud CA: **Proteasomal degradation restricts the nuclear lifespan of AID**. *J Exp Med* 2008, **205**:1357-1368.

15. Patenaude AM, Orthwein A, Hu Y, Campo VA, Kavli B, Buschiazzo A, Di Noia JM: **Active nuclear import and cytoplasmic retention of activation-induced deaminase**. *Nat Struct Mol Biol* 2009, **16**:517-527.

16. Geisberger R, Rada C, Neuberger MS: **The stability of AID and its function in class-switching are critically sensitive to the identity of its nuclear-export sequence**. *Proc Natl Acad Sci USA* 2009, **106**:6736-6741.

17. Casellas R, Yamane A, Kovalchuk AL, Potter M: **Restricting activation-induced cytidine deaminase tumorigenic activity in B lymphocytes**. *Immunology* 2009, **126**:316-328.

18. Ito S, Nagaoka H, Shinkura R, Begum N, Muramatsu M, Nakata M, Honjo T: **Activation-induced cytidine deaminase shuttles between nucleus and cytoplasm like apolipoprotein B mRNA editing catalytic polypeptide 1**. *Proc Natl Acad Sci USA* 2004, **101**:1975-1980.

19. Muramatsu M, Sankaranand VS, Anant S, Sugai M, Kinoshita K, Davidson NO, Honjo T: **Specific expression of activation-induced cytidine deaminase (AID), a novel member of the RNA-editing deaminase family in germinal center B cells**. *J Biol Chem* 1999, **274**:18470-18476.

20. Muto T, Muramatsu M, Taniwaki M, Kinoshita K, Honjo T: **Isolation, tissue distribution, and chromosomal localization of the human activation-induced cytidine deaminase (AID) gene**. *Genomics* 2000, **68**:85-88.

21. Matsumoto Y, Marusawa H, Kinoshita K, Endo Y, Kou T, Morisawa T, Azuma T, Okazaki IM, Honjo T, Chiba T: ***Helicobacter pylori* infection triggers aberrant expression of activation-induced cytidine deaminase in gastric epithelium**. *Nat Med* 2007, **13**:470-476.

22. Hatakeyama M: ***Helicobacter pylori* and gastric carcinogenesis**. *J Gastroenterol* 2009, **44**:239-248.

23. Viala J, Chaput C, Boneca IG, Cardona A, Girardin SE, Moran AP, Athman R, Memet S, Huerre MR, Coyle AJ *et al.*: **Nod1 responds to peptidoglycan delivered by the *Helicobacter pylori* cag pathogenicity island**. *Nat Immunol* 2004, **5**:1166-1174.

24. Crouch EE, Li Z, Takizawa M, Fichtner-Feigl S, Gourzi P, Montano C, Feigenbaum L, Wilson P, Janz S, Papavasiliou FN *et al.*: **Regulation of AID expression in the immune response**. *J Exp Med* 2007, **204**:1145-1156.

25. Yadav A, Olaru A, Saltis M, Setren A, Cerny J, Livak F: **Identification of a ubiquitously active promoter of the murine activation-induced cytidine deaminase (AICDA) gene**. *Mol Immunol* 2006, **43**:529-541.

26. Park SR, Zan H, Pal Z, Zhang J, Al-Qahtani A, Pone EJ, Xu Z, Mai T, Casali P: **HoxC4 binds to the promoter of the cytidine deaminase AID gene to induce AID expression, class-switch DNA recombination and somatic hypermutation**. *Nat Immunol* 2009, **10**:540-550.

27. Tran TH, Nakata M, Suzuki K, Begum NA, Shinkura R, Fagarasan S, Honjo T, Nagaoka H: **B cell-specific and stimulation-responsive enhancers derepress Aicda by overcoming the effects of silencers**. *Nat Immunol* 2010, **11**:148-154.

28. Dedeoglu F, Horwitz B, Chaudhuri J, Alt FW, Geha RS: **Induction of activation-induced cytidine deaminase gene expression by IL-4 and CD40 ligation is dependent on STAT6 and NFkappaB**. *Int Immunol* 2004, **16**:395-404.

29. •• Liu M, Duke JL, Richter DJ, Vinuesa CG, Goodnow CC, Kleinstein SH, Schatz DG: **Two levels of protection for the B cell genome during somatic hypermutation**. *Nature* 2008, **451**:841-845.
By extensive sequencing of murine B cell genes, the authors demonstrate that AID acts broadly on the genome and approximately 25% of expressed genes analyzed in this study accumulated mutations possibly induced by AID activity in germinal center B cells.

30. Robbiani DF, Bothmer A, Callen E, Reina-San-Martin B, Dorsett Y, Difilippantonio S, Bolland DJ, Chen HT, Corcoran AE, Nussenzweig A *et al.*: **AID is required for the chromosomal breaks in c-myc that lead to c-myc/IgH translocations**. *Cell* 2008, **135**:1028-1038.

31. • Robbiani DF, Bunting S, Feldhahn N, Bothmer A, Camps J, Deroubaix S, McBride KM, Klein IA, Stone G, Eisenreich TR *et al.*: **AID produces DNA double-strand breaks in non-Ig genes and mature B cell lymphomas with reciprocal chromosome translocations**. *Mol Cell* 2009, **36**:631-641.
Demonstration of the capacity of AID to produce paired DNA double-strand break throughout the genome that can lead to lymphoma-associated chromosome translocation in mature B cells.

32. Okazaki IM, Hiai H, Kakazu N, Yamada S, Muramatsu M, Kinoshita K, Honjo T: **Constitutive expression of AID leads to tumorigenesis**. *J Exp Med* 2003, **197**:1173-1181.

33. Morisawa T, Marusawa H, Ueda Y, Iwai A, Okazaki IM, Honjo T, Chiba T: **Organ-specific profiles of genetic changes in cancers caused by activation-induced cytidine deaminase expression**. *Int J Cancer* 2008, **123**:2735-2740.

34. Isaacson P, Wright DH: **Malignant lymphoma of mucosa-associated lymphoid tissue. A distinctive type of B-cell lymphoma**. *Cancer* 1983, **52**:1410-1416.

35. Zucca E, Bertoni F, Roggero E, Cavalli F: **The gastric marginal zone B-cell lymphoma of MALT type**. *Blood* 2000, **96**:410-419.

36. Suarez F, Lortholary O, Hermine O, Lecuit M: **Infection-associated lymphomas derived from marginal zone B cells: a model of antigen-driven lymphoproliferation**. *Blood* 2006, **107**:3034-3044.

37. Isaacson PG, Du MQ: **MALT lymphoma: from morphology to molecules**. *Nat Rev Cancer* 2004, **4**:644-653.

38. Parsonnet J, Hansen S, Rodriguez L, Gelb AB, Warnke RA, Jellum E, Orentreich N, Vogelman JH, Friedman GD: ***Helicobacter pylori* infection and gastric lymphoma**. *N Engl J Med* 1994, **330**:1267-1271.

39. Zullo A, Hassan C, Andriani A, Cristofari F, De Francesco V, Ierardi E, Tomao S, Morini S, Vaira D: **Eradication therapy for *Helicobacter pylori* in patients with gastric MALT lymphoma: a pooled data analysis**. *Am J Gastroenterol* 2009, **104**:1932-1937 quiz 1938.

40. Wotherspoon AC, Doglioni C, Diss TC, Pan L, Moschini A, de Boni M, Isaacson PG: **Regression of primary low-grade B-cell gastric lymphoma of mucosa-associated lymphoid**

tissue type after eradication of *Helicobacter pylori*. *Lancet* 1993, **342**:575-577.

41. Greeve J, Philipsen A, Krause K, Klapper W, Heidorn K, Castle BE, Janda J, Marcu KB, Parwaresch R: **Expression of activation-induced cytidine deaminase in human B-cell non-Hodgkin lymphomas.** *Blood* 2003, **101**:3574-3580.

42. • Pasqualucci L, Bhagat G, Jankovic M, Compagno M, Smith P, Muramatsu M, Honjo T, Morse HC 3rd, Nussenzweig MC, Dalla-Favera R: **AID is required for germinal center-derived lymphomagenesis.** *Nat Genet* 2008, **40**:108-112.
By crossing the mouse model of B cell lymphoma with the AID deficient mouse, the authors showed that AID deficiency prevents Bcl6-dependent, germinal center-derived B cell lymphomas.

43. Bombardieri M, Barone F, Humby F, Kelly S, McGurk M, Morgan P, Challacombe S, De Vita S, Valesini G, Spencer J *et al.*: **Activation-induced cytidine deaminase expression in follicular dendritic cell networks and interfollicular large B cells supports functionality of ectopic lymphoid neogenesis in autoimmune sialoadenitis and MALT lymphoma in Sjogren's syndrome.** *J Immunol* 2007, **179**:4929-4938.

44. Deutsch AJ, Aigelsreiter A, Staber PB, Beham A, Linkesch W, Guelly C, Brezinschek RI, Fruhwirth M, Emberger W, Buettner M *et al.*: **MALT lymphoma and extranodal diffuse large B-cell lymphoma are targeted by aberrant somatic hypermutation.** *Blood* 2007, **109**:3500-3504.

45. Delker RK, Fugmann SD, Papavasiliou FN: **A coming-of-age story: activation-induced cytidine deaminase turns 10.** *Nat Immunol* 2009, **10**:1147-1153.

46. Marusawa H: **Aberrant AID expression and human cancer development.** *Int J Biochem Cell Biol* 2008, **40**:1399-1402.

47. Endo Y, Marusawa H, Kinoshita K, Morisawa T, Sakurai T, Okazaki IM, Watashi K, Shimotohno K, Honjo T, Chiba T: **Expression of activation-induced cytidine deaminase in human hepatocytes via NF-kappaB signaling.** *Oncogene* 2007, **26**:5587-5595.

48. •• Takai A, Toyoshima T, Uemura M, Kitawaki Y, Marusawa H, Hiai H, Yamada S, Okazaki IM, Honjo T, Chiba T *et al.*: **A novel mouse model of hepatocarcinogenesis triggered by AID causing deleterious p53 mutations.** *Oncogene* 2008.
Pioneering study demonstrating the crucial role of mutational accumulation in immature stem cells on the development of cancer cells. The authors show that constitutive AID expression in cells producing a marker of immature hepatocytes resulted in the appearance of hepatocellular carcinoma.

49. Komori J, Marusawa H, Machimoto T, Endo Y, Kinoshita K, Kou T, Haga H, Ikai I, Uemoto S, Chiba T: **Activation-induced cytidine deaminase links bile duct inflammation to human cholangiocarcinoma.** *Hepatology* 2008, **47**:888-896.

50. • Endo Y, Marusawa H, Kou T, Nakase H, Fujii S, Fujimori T, Kinoshita K, Honjo T, Chiba T: **Activation-induced cytidine deaminase links between inflammation and the development of colitis-associated colorectal cancers.** *Gastroenterology* 2008, **135**: 889-898, e881-883.
The authors show that AID expression in human colonic epithelial cells is induced in response to Th2-driven cytokines IL-4 and IL-13, which are activated in inflammatory bowel disease. This is the first study to provide the possible link between colonic inflammation, AID expression and colorectal cancer development.

51. Aoi T, Marusawa H, Sato T, Chiba T, Maruyama M: **Risk of subsequent development of gastric cancer in patients with previous gastric epithelial neoplasia.** *Gut* 2006, **55**:588-589.

Individualized Extension of Pegylated Interferon Plus Ribavirin Therapy for Recurrent Hepatitis C Genotype 1b After Living-Donor Liver Transplantation

Yoshihide Ueda,[1,3] Yasutsugu Takada,[2] Hiroyuki Marusawa,[1] Hiroto Egawa,[2] Shinji Uemoto,[2] and Tsutomu Chiba[1]

Background. The efficacy of combination therapy with pegylated interferon and ribavirin for recurrent hepatitis C genotype 1 after liver transplantation is limited. In this study, we designed an individualized treatment regimen with pegylated interferon and ribavirin for recurrent hepatitis C based on individual viral responses.
Methods. Thirty-four patients with recurrent hepatitis C genotype 1b after living-donor liver transplantation received combination therapy with pegylated interferon α-2b and ribavirin. Treatment was continued for an additional 12 months after serum hepatitis C virus (HCV) RNA became undetectable.
Results. Of the 34 patients, 18 became negative for serum HCV RNA within 12 months (range, 1.2–9.9 months; median, 4.0 months). The treatment for the 18 patients was individualized by adding a further 12 months of treatment after the disappearance of serum HCV RNA, resulting in treatment durations of 13.2 to 21.9 months (median, 16.0 months). Notably, 17 (94%) of the 18 patients who received the individualized extended treatment achieved sustained virologic response (SVR), resulting in a 50% SVR rate. Six patients (18%) discontinued the treatment, but none of the 18 patients who received the extended protocol withdrew from the study.
Conclusions. Individualized extension of combination therapy with pegylated interferon and ribavirin for recurrent hepatitis C after liver transplantation resulted in a high SVR rate and good tolerability.

Keywords: Hepatitis C, Liver transplantation, Extended treatment, Pegylated interferon, Ribavirin.

(*Transplantation* 2010;90: 661–665)

Hepatitis C virus (HCV) infection is the predominant cause of cirrhosis and hepatocellular carcinoma in Japan, the United States, and western Europe. End-stage liver disease caused by HCV infection is the main indication for liver transplantation. However, almost all patients who receive liver transplantation for HCV-related liver disease develop recurrent infection, and 70% to 90% of patients suffer from histologically proven recurrent hepatitis (*1–6*). The progression of recurrent hepatitis C is often accelerated, and without appropriate antiviral therapy, 10% to 25% of patients develop cirrhosis within 5 years of transplantation, resulting in poorer prognosis for HCV-positive recipients than for HCV-negative recipients (*7*). The median interval from transplantation to cirrhosis is 10 years for transplant patients, compared with that of 20 to 40 years for nontransplant patients (*8*).

To prevent the progression of hepatitis C after liver transplantation, combination therapy with pegylated interferon and ribavirin is commonly administered for 12 months (*9, 10*). However, the efficacy of this combination therapy is limited, especially for patients infected with HCV genotype 1. A systematic review of studies on combination therapy with pegylated interferon and ribavirin for recurrent hepatitis C after liver transplantation showed that the mean sustained virologic response (SVR) rate among patients infected with HCV genotype 1 was only 28.7% (range, 12.5%–40%) (*11*). In contrast, the mean end-of-treatment virologic response was 42.2% (range, 17%–68%), indicating that virologic relapse was a major cause of the low SVR rate. Therefore, it is necessary to develop a new strategy for reducing the incidence of relapse if the SVR rate is to be increased.

Recently, trials have been conducted to evaluate whether the SVR rate in nontransplant patients with chronic

This work was supported by Grants-in-aid for Scientific Research 19790480 from the Ministry of Education, Culture, Sports, Science and Technology of Japan.

[1] Department of Gastroenterology and Hepatology, Graduate School of Medicine, Kyoto University, Shogoin, Sakyo-ku, Kyoto, Japan.
[2] Department of Surgery, Graduate School of Medicine, Kyoto University, Shogoin, Sakyo-ku, Kyoto, Japan.
[3] Address correspondence to: Yoshihide Ueda, M.D., Ph.D., Department of Gastroenterology and Hepatology, Graduate School of Medicine, Kyoto University, Shogoin, Sakyo-ku, Kyoto, Japan.

Y. Ueda participated in research design, the performance of the research, data analysis, and the writing of the paper; Y. Takada, H. Marusawa, and H. Egawa participated in the performance of the research; and S. Uemoto and T. Chiba participated in research design and manuscript review.

E-mail: yueda@kuhp.kyoto-u.ac.jp

Received 17 December 2009.
Accepted 3 January 2010.

ISSN 0041-1337/10/9006-661
DOI: 10.1097/TP.0b013e3181d2bfca

hepatitis C genotype 1 can be improved by extending the duration of treatment (*12–17*). These trials indicated that extension of treatment from 48 to 72 weeks significantly increased the SVR rate in patients with a delayed virologic response. However, because the virologic response to the treatment varies between patients, especially between transplant recipients who frequently require dose reduction, it is desirable to individualize the treatment regimen to achieve SVR more efficiently.

In this study, we designed an individualized treatment regimen in which combination therapy with pegylated interferon α-2b and ribavirin was continued in patients for an additional 12 months after serum HCV RNA became undetectable, and the efficacy of this extended treatment in patients with recurrent hepatitis C genotype 1b who had undergone living-donor liver transplantation (LDLT) was evaluated.

EXPERIMENTAL PROCEDURES

Patients

Between February 2006 and February 2008, 40 patients were evaluated for antiviral treatment after undergoing LDLT for HCV-related liver diseases caused by HCV genotype 1b infection at the Kyoto University, and 34 patients were diagnosed as having recurrent hepatitis C. Of the 34 patients, five patients had previously been treated with interferon plus ribavirin after liver transplantation and did not achieve an SVR (*18*). Combination therapy with pegylated interferon and ribavirin was administered to the 34 patients. Eligibility criteria for the treatment were positivity for serum HCV RNA and histologic evidence of recurrent hepatitis C. Patients with a necroinflammatory activity classification of A2 or greater or a fibrosis stage of F1 or greater (METAVIR score) were treated. Exclusion criteria were a neutrophil count of less than 750/μL, a platelet count of less than 40,000/μL, a hemoglobin level of less than or equal to 9.0 g/dL, and renal insufficiency (serum creatinine levels >2 mg/dL).

Treatment Protocol and Definition of Responses to Treatment

The treatment protocol for patients with recurrent hepatitis C after liver transplantation consisted of 1.5 μg/kg of pegylated interferon α-2b once weekly plus ribavirin at an oral dose of 600 mg/day (body weight <60 kg) or 800 mg/day (body weight >60 kg). Patients who became negative for serum HCV RNA within 12 months of initiation of the combination therapy were enrolled in the individualized treatment protocol, which started when patients first became negative for serum HCV RNA and ended 12 months thereafter. The overall duration of treatment was defined as the sum of the period that elapsed before disappearance of serum HCV RNA plus 12 months for individualized treatment after the disappearance of serum HCV RNA (e.g., if serum HCV RNA became negative after 3 months, the total treatment duration was 15 months). Patients who were negative for serum HCV RNA for more than 6 months after completion of interferon therapy were defined as showing an SVR. If serum HCV RNA was positive after 12 months, the treatment protocol was discontinued and the patient was classified as having shown no response.

The dose of pegylated interferon was reduced to 0.75 μg/kg if the neutrophil count was less than 750/μL or the platelet count was less than 75,000/μL, and pegylated interferon was discontinued if the neutrophil count was less than 500/μL or the platelet count was less than 50,000/μL. The ribavirin dose was reduced to 400 mg/day if the hemoglobin level was less than 10 g/dL and to 200 mg/day if the hemoglobin level was less than 9 g/dL. Ribavirin was discontinued if the hemoglobin level was less than 8 g/dL. Granulocyte colony-stimulating factor (lenograstim, 100 μg/week) was used for neutrophil counts below 500/μL and was continued until values returned to more than 750/μL. Recombinant erythropoietin (epoetin beta, 6000 IU/week) was started if the hemoglobin level was less than 8 g/dL and was continued until it became more than 9 g/dL. Granulocyte colony-stimulating factor was used for two patients, and erythropoietin was given in four patients (Table 1).

Immunosuppression

The standard immunosuppression protocol consisted of tacrolimus and low-dose steroid therapy (*18*). The lower limit of the target for whole blood tacrolimus level was 10 to 15 ng/mL during the first 2 weeks, 10 ng/mL thereafter, and 5 to 8 ng/mL from the second month onward. Cyclosporine microemulsion was administered instead of tacrolimus to induce immunosuppression in four patients (Table 1). Steroid therapy was initiated at a dose of 10 mg/kg before graft reperfusion and then tapered down from 1 mg/kg per day on the first day to 0.3 mg/kg per day until the end of the first month, followed by 0.1 mg/kg per day until the end of the third month. Subsequently, steroid administration was terminated. Mycophenolate mofetil was administered to patients who experienced refractory rejection or required reduction of the tacrolimus or cyclosporine dose because of adverse events.

Virologic Assays and Histologic Assessment

HCV genotype was determined using a genotyping system based on polymerase chain reaction (PCR) of the core region using genotype-specific PCR primers (*19*). Serum HCV RNA load was evaluated once a month during treatment and at 6 months of follow-up after treatment using PCR and an Amplicor HCV assay (Cobas Amplicor HCV Monitor, Roche Molecular Systems, Pleasanton, CA).

Liver biopsies were evaluated if a patient had liver enzyme levels greater than twice the normal upper limit or at yearly intervals with informed consent. Necroinflammatory activity (A0–A3) and fibrosis stage (F0–F4) were assessed using the METAVIR score (*20, 21*).

Statistical Analysis

Characteristics of the patients were described and compared between patients with an SVR and patients who did not achieve an SVR (non-SVR). For continuous variables, medians and ranges are given, and the data were analyzed by the Wilcoxon test. For categorical variables, counts are given, and the data were analyzed by chi-square test. $P<0.05$ was considered significant.

TABLE 1. Characteristics of 34 patients treated with pegylated interferon and ribavirin after LDLT

	Total (n=34)	SVR (n=17)	Non-SVR (n=17)	P
Age (yr)	58 (21–68)	58 (21–68)	57 (50–66)	0.760[a]
Males/females	19/15	10/7	9/8	0.730[b]
Time since LDLT (mo)	8.0 (3.1–150.9)	7.8 (3.1–150.9)	9.0 (3.2–67.9)	0.760[a]
HCV RNA (kIU/mL)	4145 (387–5000<)	3230 (834–5000<)	5000 (387–5000<)	0.099[a]
White blood cell count (per microliters)	5100 (1700–9900)	4900 (2200–8300)	5500 (1700–9900)	0.786[a]
Neutrophil (per microliters)	2520 (830–6230)	2630 (1240–6230)	2450 (830–3810)	0.204[a]
Hemoglobin (g/dL)	12.0 (9.2–16.4)	11.6 (9.7–16.4)	12.0 (9.2–14.8)	0.786[a]
Platelet (10^4/μL)	23.8 (4.3–46.7)	23.9 (6.1–46.7)	20.6 (4.3–39.2)	0.274[a]
AST (IU/L)	78 (25–308)	79 (30–230)	68 (25–308)	0.973[a]
ALT (IU/L)	65 (21–392)	64 (28–216)	66 (21–392)	0.812[a]
ALP (IU/L)	446 (204–1583)	431 (204–1583)	468 (279–1533)	0.306[a]
γ-GTP (IU/L)	99 (23–1282)	124 (23–425)	74 (27–1282)	0.413[a]
Bilirubin (mg/dL)	0.9 (0.4–2.6)	0.8 (0.7–1.7)	0.9 (0.4–2.6)	0.540[a]
METAVIR score				
A 0/1/2/3	0/19/13/2	0/9/7/1	0/10/6/1	0.937[b]
F 0/1/2/3/4	3/24/7/0/0	0/14/3/0/0	3/10/4/0/0	0.149[b]
Immunosuppression				0.252[b]
Tacrolimus	14	6	8	
Tacrolimus+MMF	13	7	6	
Tacrolimus+prednisolone	3	3	0	
Cyclosporine	2	1	1	
Cyclosporine+MMF	2	0	2	
Trough level for tacrolimus (ng/mL)	6.1 (2.2–10.9)	6.1 (2.2–9.5)	6.2 (3.3–10.9)	0.667[a]
Dose modification of peginterferon	14	3	11	0.005[b]
Dose modification of ribavirin	27	11	16	0.034[b]
Use of G-CSF	2	0	2	0.145[b]
Use of erythropoietin	4	1	3	0.287[b]

Qualitative variables are shown in number; and quantitative variables are expressed as median (range).
[a] Wilcoxon test.
[b] χ^2 test.
AST, aspartate aminotransferase; ALT, alanine aminotransferase; ALP, alkaline phosphatase; γ-GTP, γ-glutamyl transpeptidase; MMF, mycophenolate mofetil; G-CSF, granulocyte colony-stimulating factor; LDLT, living-donor liver transplant; SVR, sustained virologic response.

RESULTS

Baseline Characteristics of Patients

We studied the baseline clinical and virologic characteristics of the 34 patients before initiation of pegylated interferon plus ribavirin therapy (Table 1). The median age of the patients at the beginning of the therapy was 58 years (range, 21–68 years). The treatment started at a median of 8.0 months (range, 3.1–150.9 months) after liver transplantation. All patients were infected with HCV genotype 1b. Median serum HCV RNA load was 4145 kIU/mL (range, 387–5000 kIU/mL), that is, most patients had an extremely high viral load. Before treatment, all patients showed necroinflammatory activity greater than A1, and 31 patients (91%) had a fibrosis score greater than F1 (METAVIR score).

Efficacy of Combination Therapy With Pegylated Interferon and Ribavirin

We studied the outcomes of the combination therapy given to 34 patients with recurrent hepatitis C genotype 1b after LDLT (Fig. 1). Serum HCV RNA became undetectable within 12 months in 18 patients (53%). The median interval between the time at which treatment was initiated and the time at which serum HCV RNA became undetectable was 4.0 months (range, 1.2–9.9 months). For these 18 patients, treatment was continued for an additional 12 months after serum HCV RNA became undetectable, resulting in a median treatment duration of 16.0 months (range, 13.2–21.9 months). Notably, 17 (94%) of these 18 patients achieved SVR. In 10 patients (29%), HCV RNA was detectable in the serum 12 months after the initiation of the treatment, and these patients were defined as having no response. For the 34 patients, including six who discontinued treatment, the SVR rate was 50%. No significant difference in baseline characteristics between 17 patients who achieved an SVR and 17 patients who did not achieve an SVR (non-SVR) was demonstrated (Table 1).

Liver biopsy was performed for 12 of the 34 patients, including six with an SVR and six with a non-SVR, at 12 to 24 months after the initiation of the treatment. Median durations from initiation of treatment to liver biopsy were 15.6 months (range, 14.7–17.5 months) in SVR group and 18.1 months (range, 12.0–21.1 months) in non-SVR group. Table 2 demonstrates the changes in histologic activity and fi-

Copyright © Lippincott Williams & Wilkins. Unauthorized reproduction of this article is prohibited.

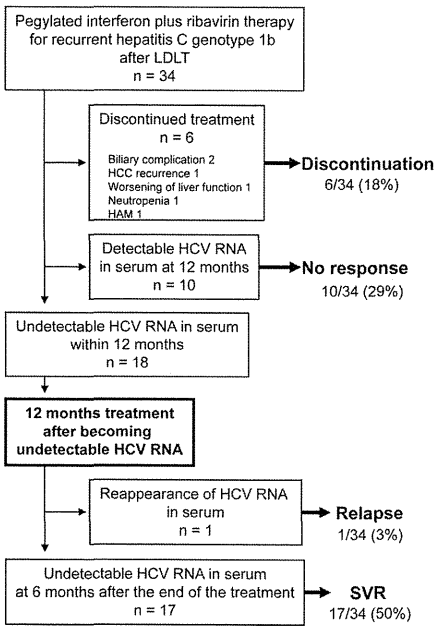

FIGURE 1. Flow diagram showing the outcome of extended pegylated interferon plus ribavirin therapy for patients with recurrent hepatitis C genotype 1b after living-donor liver transplantation. HCC, hepatocellular carcinoma; HAM, human T-lymphotropic virus (HTLV-1)-associated myelopathy; SVR, sustained virologic response.

TABLE 2. Numbers of the patients showing changes in activity grade and fibrosis score (METAVIR score) at 12 to 24 months after the initiation of treatment

	Activity		Fibrosis	
	SVR (n=6)	Non-SVR (n=6)	SVR (n=6)	Non-SVR (n=6)
Improvement	3	4	1	0
No change	3	2	5	4
Worsening	0	0	0	2

SVR, sustained virologic response.

brosis of individual patients. Activity grade of all patients in both the SVR group and the non-SVR group improved or remained stable. Fibrosis stage was deteriorated in two of six patients in the non-SVR group, whereas no patients with an SVR showed worsening of fibrosis. There was no significant difference in histologic changes of both activity grade (P=0.558) and fibrosis stage (P=0.211) between the SVR and non-SVR groups during the short-term follow-up.

Safety and Tolerability

Six patients (18%) discontinued the treatment because of biliary complications (n=2), recurrent hepatocellular carcinoma (n=1), worsening of liver function (n=1), neutropenia (n=1), and human T-cell lymphotropic virus–associated myelopathy (n=1). The patient who discontinued the treatment because of worsening of liver function 9 months after starting the treatment was diagnosed with chronic rejection by liver biopsy 1 month after the discontinuation and died 2 months after the diagnosis. None of the 18 patients who received the extended treatment withdrew from the study. For the 28 patients who continued the treatment for 12 months or more, modification of the pegylated interferon or ribavirin dose was required in 22 patients (79%), reduction in the pegylated interferon dose was required in eight (29%), and reduction in the ribavirin dose was required in 21 (75%). During the extended treatment of the 18 patients, the ribavirin dose needed to be reduced for only three patients, and the pegylated interferon dose did not need to be reduced for any patient. Rate of the patients who required dose modifications of pegylated interferon and ribavirin was significantly higher in the non-SVR group than in the SVR group (Table 1).

DISCUSSION

In this study, an SVR rate of 50% was achieved using individualized extension of combination therapy with pegylated interferon α-2b and ribavirin for patients with recurrent hepatitis C genotype 1b after LDLT. This SVR rate was higher than that achieved in previous studies in which liver transplant recipients were treated for 12 months (*9–11*). Notably, only one patient relapsed in this study, indicating that individualized extension of treatment reduces the relapse rate and increases the SVR rate.

The virologic response during treatment is useful for predicting whether SVR will be achieved. In both transplant recipients and nontransplant patients, failure to achieve an early virologic response (EVR) to combination therapy, which was defined as a less than or equal to 2-log reduction in (partial EVR) or the complete absence of serum HCV RNA (complete EVR) at week 12 of therapy compared with the baseline level, most accurately predicts that SVR will not be achieved (*11, 22*). For nontransplant patients who do not achieve complete EVR, treatment can be extended to 72 weeks instead of 48 weeks (*13, 16, 17*). In this study, complete EVR was achieved in only six patients. For the other 12 patients with delayed virologic responses, we believed it was desirable to extend the treatment to achieve SVR. However, it seems unlikely that a uniform duration of treatment can be defined, because virologic responses to combination therapy vary between transplant recipients who require frequent dose modifications and have high initial viral loads. In fact, in this study, there was a considerable variation in the time required for serum HCV RNA to become undetectable in different patients. Of the 18 patients who received the extended treatment, serum HCV RNA became undetectable within 12 weeks in six patients (33%), between 12 and 24 weeks in six patients (33%), between 24 and 36 weeks in three patients (17%), and after 36 weeks of treatment in three patients (17%). Therefore, individualized extension of the treatment would be the best strategy for these patients. The results of individualized treatment of nontransplant patients with chronic hepatitis C were recently reported (*15*). Treatment for 44 weeks after serum HCV RNA became undetectable in nontransplant patients with chronic hepatitis C genotype 1 resulted in a significantly higher SVR rate than that in 48 weeks of standard therapy. Although the optimum duration of treatment for hepatitis C after liver transplantation is unknown, individualized treatment based on the time required for serum HCV RNA to become undetectable could help define the optimum duration.

Another issue involving antiviral therapy after transplantation is the tolerability of pegylated interferon and ribavirin. Dose reductions are frequent and drug discontinuation rates are higher in transplant patients than in nontransplant patients. In previous studies, 39% and 54% of patients received reduced doses of pegylated interferon and ribavirin, respectively, and the pooled weighted rate of treatment discontinuation was 26% (*11*). Therefore, treatment is often limited by poor tolerability and the frequent need for dose reductions and discontinuation (*10, 11*). In this study, 10 patients needed to discontinue treatment, but the reasons for this were not directly associated with the treatment in 9 of the 10 patients. All these patients were excluded within 12 months, showing that the extended protocol did not increase the incidence of major adverse events. Dose modifications were required for most patients, mainly because of cytopenia, but complications caused by cytopenia were not observed. Thus, the extended treatment did not affect the safety and tolerability of the therapy in this study.

In conclusion, individualized extension of combination therapy with pegylated interferon α-2b and ribavirin resulted in a high SVR rate and good tolerability. Further studies with a large number of patients are required to determine the efficacy and safety of this extended treatment regimen for recurrent hepatitis C after liver transplantation.

REFERENCES

1. Berenguer M, Prieto M, San Juan F, et al. Contribution of donor age to the recent decrease in patient survival among HCV-infected liver transplant recipients. *Hepatology* 2002; 36: 202.
2. Feray C, Caccamo L, Alexander GJ, et al. European collaborative study on factors influencing outcome after liver transplantation for hepatitis C. European Concerted Action on Viral Hepatitis (EUROHEP) Group. *Gastroenterology* 1999; 117: 619.
3. Forman LM, Lewis JD, Berlin JA, et al. The association between hepatitis C infection and survival after orthotopic liver transplantation. *Gastroenterology* 2002; 122: 889.
4. Gane E. The natural history and outcome of liver transplantation in hepatitis C virus-infected recipients. *Liver Transpl* 2003; 9: S28.
5. Prieto M, Berenguer M, Rayon JM, et al. High incidence of allograft cirrhosis in hepatitis C virus genotype 1b infection following transplantation: relationship with rejection episodes. *Hepatology* 1999; 29: 250.
6. Sanchez-Fueyo A, Restrepo JC, Quinto L, et al. Impact of the recurrence of hepatitis C virus infection after liver transplantation on the long-term viability of the graft. *Transplantation* 2002; 73: 56.
7. Velidedeoglu E, Mange KC, Frank A, et al. Factors differentially correlated with the outcome of liver transplantation in hcv+ and HCV− recipients. *Transplantation* 2004; 77: 1834.
8. Berenguer M, Ferrell L, Watson J, et al. HCV-related fibrosis progression following liver transplantation: Increase in recent years. *J Hepatol* 2000; 32: 673.
9. Gordon FD, Kwo P, Vargas HE. Treatment of hepatitis C in liver transplant recipients. *Liver Transpl* 2009; 15: 126.
10. Terrault NA. Hepatitis C therapy before and after liver transplantation. *Liver Transpl* 2008; 14(suppl 2): S58.
11. Berenguer M. Systematic review of the treatment of established recurrent hepatitis C with pegylated interferon in combination with ribavirin. *J Hepatol* 2008; 49: 274.
12. Akuta N, Suzuki F, Hirakawa M, et al. A matched case-controlled study of 48 and 72 weeks of peginterferon plus ribavirin combination therapy in patients infected with HCV genotype 1b in Japan: Amino acid substitutions in HCV core region as predictor of sustained virological response. *J Med Virol* 2009; 81: 452.
13. Berg T, von Wagner M, Nasser S, et al. Extended treatment duration for hepatitis C virus type 1: Comparing 48 versus 72 weeks of peginterferon-alfa-2a plus ribavirin. *Gastroenterology* 2006; 130: 1086.
14. Buti M, Valdes A, Sanchez-Avila F, et al. Extending combination therapy with peginterferon alfa-2b plus ribavirin for genotype 1 chronic hepatitis C late responders: A report of 9 cases. *Hepatology* 2003; 37: 1226.
15. Ide T, Hino T, Ogata K, et al. A randomized study of extended treatment with peginterferon alpha-2b plus ribavirin based on time to HCV RNA negative-status in patients with genotype 1b chronic hepatitis C. *Am J Gastroenterol* 2009; 104: 70.
16. Pearlman BL, Ehleben C, Saifee S. Treatment extension to 72 weeks of peginterferon and ribavirin in hepatitis c genotype 1-infected slow responders. *Hepatology* 2007; 46: 1688.
17. Sanchez-Tapias JM, Diago M, Escartin P, et al. Peginterferon-alfa2a plus ribavirin for 48 versus 72 weeks in patients with detectable hepatitis C virus RNA at week 4 of treatment. *Gastroenterology* 2006; 131: 451.
18. Ueda Y, Takada Y, Haga H, et al. Limited benefit of biochemical response to combination therapy for patients with recurrent hepatitis C after living-donor liver transplantation. *Transplantation* 2008; 85: 855.
19. Ohno O, Mizokami M, Wu RR, et al. New hepatitis C virus (HCV) genotyping system that allows for identification of HCV genotypes 1a, 1b, 2a, 2b, 3a, 3b, 4, 5a, and 6a. *J Clin Microbiol* 1997; 35: 201.
20. Bedossa P, Poynard T. An algorithm for the grading of activity in chronic hepatitis C. The METAVIR Cooperative Study Group. *Hepatology* 1996; 24: 289.
21. Poynard T, Bedossa P, Opolon P. Natural history of liver fibrosis progression in patients with chronic hepatitis C. The OBSVIRC, METAVIR, CLINIVIR, and DOSVIRC groups. *Lancet* 1997; 349: 825.
22. Ghany MG, Strader DB, Thomas DL, et al. Diagnosis, management, and treatment of hepatitis C: An update. *Hepatology* 2009; 49: 1335.

Copyright © Lippincott Williams & Wilkins. Unauthorized reproduction of this article is prohibited.

JOURNAL OF VIRAL HEPATITIS JVH

Journal of Viral Hepatitis, 2010, 17, 481–487 doi:10.1111/j.1365-2893.2009.01207.x

Clinical features of biochemical cholestasis in patients with recurrent hepatitis C after living-donor liver transplantation

Y. Ueda,[1] Y. Takada,[2] H. Marusawa,[1] H. Haga,[3] T. Sato,[4] Y. Tanaka,[1] H. Egawa,[2] S. Uemoto[2] and T. Chiba[1]

[1]*Department of Gastroenterology and Hepatology;* [2]*Department of Surgery;* [3]*Department of Pathology, Graduate School of Medicine, Kyoto University, Kyoto; and* [4]*Department of Biostatistics, Kyoto University School of Public Health, Kyoto, Japan*

Received February 2009; accepted for publication July 2009

SUMMARY. Recurrent hepatitis C after liver transplantation (HepC-LT) progresses faster than hepatitis C in non-transplant settings. Cholestasis has been suggested to be one characteristic of HepC-LT related to the rapid progression. We investigated the clinical features of biochemical cholestasis, which we defined as high serum concentrations of alkaline phosphatase and γ-glutamyl transpeptidase, in patients with recurrent hepatitis C after living-donor liver transplantation. Eighty patients were diagnosed with post-transplant recurrent hepatitis C after exclusion of other aetiologies of cholestasis by liver biopsy and imaging. The clinical features of biochemical cholestasis in the patients with HepC-LT, including histological changes, the efficacy of interferon therapy and helper T-cell (Th) subsets in the peripheral blood, were analysed. Fifty-five of the 80 patients with HepC-LT (69%) had evidence of biochemical cholestasis. Progression of liver fibrosis to stage F3 or F4 was significantly accelerated in patients with biochemical cholestasis compared with patients without cholestasis. The biochemical cholestasis in patients with HepC-LT improved after interferon therapy in 22 of 39 patients (56%) who showed a virological response to the therapy, suggesting that hepatitis C virus (HCV) caused the biochemical cholestasis in these patients. Patients with biochemical cholestasis who had a biochemical response to interferon therapy showed an increased Th1 responses in peripheral blood. In conclusion, biochemical cholestasis is the characteristic feature of HepC-LT and is related to progression of liver fibrosis. An increased Th1 response is associated with cholestasis caused by HCV after liver transplantation.

Keywords: hepatitis C, cholestasis, living-donor liver transplantation, Th1.

INTRODUCTION

Liver cirrhosis caused by hepatitis C virus (HCV) is the leading indication for liver transplantation in many countries. However, almost all patients who receive liver transplantation for HCV-related liver disease develop recurrent infection, and 70–90% of patients experience histologically proven recurrent hepatitis [1–6]. Progression of recurrent hepatitis C is often accelerated, and without appropriate antiviral therapy, 10–25% of patients develop cirrhosis within 5 years after transplantation, resulting in poorer prognosis for HCV-positive than HCV-negative recipients [7]. The median interval from transplantation to cirrhosis is 10 years compared with 20–40 years in non-transplant patients [8].

The progression of recurrent hepatitis C infection after liver transplantation (HepC-LT) is poorly understood. Established factors associated with this progression and graft survival after liver transplantation are recipient-related factors including age, sex, race and severity of illness before transplantation, donor age, treatment of rejection, time to recurrence, pre-transplant and early post-transplant HCV load and cytomegalovirus infection [9,10]. Recently, Iacob *et al.* [11] reported the presence of early cholestasis as an independent negative predictor of graft and patient survival and for the development of HCV-related cirrhosis in recipients with HCV.

In addition, a small number of patients with HCV infection after liver transplantation show the unique clinical feature known as fibrosing cholestatic hepatitis (FCH) [12–14]. FCH is a progressive liver injury characterized by jaundice, high serum concentrations of alkaline phosphatase (ALP) and γ-glutamyl transpeptidase (γ-GTP), and very high serum HCV RNA levels. FCH progresses rapidly and leads to the development of cirrhosis and graft failure, sometimes within 1 year after liver transplantation. Histological findings are characterized by the presence of severe hepatocyte ballooning, intrahepatic cholestasis, pericellular and portal fibrosis, and ductular proliferation. Prognosis of FCH is poor, and antiviral therapy after the diagnosis of FCH has been reported not to improve the prognosis [15].

Even when patients do not have jaundice and intrahepatic cholestasis is not apparent in liver histology, we often encounter patients of HepC-LT with high serum concentrations of ALP and γ-GTP, which are enzymes associated with cholestasis. Elevation of ALP and/or γ-GTP in serum has been called biochemical cholestasis [16,17]. The biochemical cholestasis is rarely shown in the patients with hepatitis C in non-transplant settings (HepC-NT) [18]. Therefore, we hypothesized that biochemical cholestasis is related to the rapid progression of liver fibrosis in patients with HepC-LT. Clarification of the clinical features of the biochemical cholestasis may lead to the effective management for the patients with HepC-LT.

In this study, we retrospectively analysed the clinical features of biochemical cholestasis in the patients with HepC-LT after living-donor liver transplantation (LDLT), including the histological changes, the efficacy of interferon therapy and helper T-cell (Th) subsets in the peripheral blood.

Abbreviations: ALP, alkaline phosphatase; ALT, alanine aminotransferase; CT, computerized tomography; ERCP, endoscopic retrograde cholangiopancreatography; FCH, fibrosing cholestatic hepatitis; γ-GTP, γ-glutamyl transpeptidase; HCV, hepatitis C virus; HepC-LT, hepatitis C after liver transplantation; HepC-NT, hepatitis C in non-transplant settings; LDLT, living-donor liver transplantation; MRCP, magnetic resonance cholangiopancreatography; PCR, polymerase chain reaction; Th, helper T-cell; VR, virological response.

Correspondence: Yoshihide Ueda, Department of Gastroenterology and Hepatology, Graduate School of Medicine, Kyoto University, 54 Kawahara-cho, Shogoin, Sakyo-ku, Kyoto 606-8507, Japan.
E-mail: yueda@kuhp.kyoto-u.ac.jp

MATERIALS AND METHODS

Patients

Between March 1999 and December 2007, 141 patients with HCV-related liver diseases underwent LDLT at Kyoto University [19]. Of these, 100 patients had been followed up for more than 6 months after LDLT in our hospital. Combination therapy with interferon and ribavirin (n = 40) [20] or peginterferon and ribavirin (n = 40) was given to 80 patients with recurrent hepatitis C between January 2001 and April 2007. The remaining 20 patients did not receive anti-viral therapy because of no histological recurrence of hepatitis C in the follow-up period. Eligibility for treatment was positive serum HCV RNA and histological evidence of recurrent hepatitis C. Exclusion criteria were a neutrophil count lower than 750/μL, a platelet count lower than 40 000/μL, a haemoglobin level of 9.0 g/dL or lower, or renal insufficiency. Other aetiologies of increased alanine aminotransferase (ALT) concentration, such as rejection and biliary obstruction, were excluded by liver biopsy and imaging, including ultrasonography, computerized tomography (CT), endoscopic retrograde cholangiopancreatography (ERCP) and/or magnetic resonance cholangiopancreatography (MRCP).

To provide a comparison group for these patients, we evaluated 103 consecutive patients with HepC-NT who received combination therapy with peginterferon plus ribavirin at Kyoto University between January 2005 and April 2007. Eligibility for the treatment was positive serum HCV RNA. Liver biopsy was not performed for most patients.

Treatment protocol

The basic treatment protocol between January 2001 and April 2004 for patients with recurrent hepatitis C after liver transplantation (HepC-LT) comprised three or six mega units of interferon-α-2b three times a week plus ribavirin at 400–800 mg/day orally for the first 6 months, followed by interferon monotherapy for 6 months [20]. Combination therapy with 1.5 μg/kg of peginterferon-α-2b plus ribavirin at 400–800 mg/day orally was given between May 2004 and April 2007.

Immunosuppression

The standard immunosuppression protocol comprised tacrolimus and low-dose steroid therapy. The target for whole blood tacrolimus lower level was 10–15 ng/mL during the first 2 weeks, 10 ng/mL thereafter and 5–8 ng/mL from the second month. Cyclosporine microemulsion was administered instead of tacrolimus to induce immunosuppression in three patients. Steroid therapy was initiated at a dose of 10 mg/kg before graft reperfusion, and then tapered down from 1 mg/kg/day on the first day to 0.3 mg/kg/day until the end of the first month, followed by 0.1 mg/kg/day to the end of the third month. After that, steroid administration was terminated. Mycophenolate mofetil or mizoribine was added for patients who experienced refractory rejection or required reduction in the tacrolimus dose because of adverse events.

Virological assays

The HCV genotype was determined by a genotyping system based on polymerase chain reaction (PCR) of the core region with genotype-specific PCR primers [21]. Serum HCV RNA load was evaluated by PCR using the Amplicor HCV assay (Cobas Amplicor HCV Monitor, Roche Molecular Systems, Pleasanton, CA, USA).

Th1 and Th2 cell assay

Th1 and Th2 cell percentages were measured before interferon therapy in 27 patients with recurrent HepC-LT. Th1, Th2 and Th0 cells in the human peripheral blood T-cell population were detected by intracellular cytokine staining and flow cytometric analysis [22,23]. Peripheral blood cells from patients were stimulated with phorbol myristate acetate (10 ng/mL) and ionomycin (1 μg/mL) for 4 h in the

presence of Brefeldin A (10 μg/mL; all from Sigma Chemical Co, St Louis, MO, USA). Cells were harvested and stained with phycoerythrin (PE)-cyanin-5-conjugated-anti-CD4 monoclonal antibody (Immunotech, Marseilles, France). The cells were fixed with 1% paraformaldehyde, permeabilized with FACS Permeabilizing Solution (Becton Dickinson, San Jose, CA, USA), and stained with FITC-conjugated-anti-IFN-γ and PE-conjugated-anti-IL-4 monoclonal antibodies (Becton Dickinson). Cytokine-producing CD4-positive cells were analysed on a FACS Calibur (BD Biosciences, San Jose, CA, USA). The percentages of cells in the gate of IFN-γ^+ IL-4^- cells (Th1), IFN-γ^- IL4^+ cells (Th2), IFN-γ^+ IL-4^+ cells (double-positive Th0 or Th0-DP) and IFNγ^- IL-4^- cells (double-negative Th0 or Th0-DN) were analysed.

Histological assessment

Liver biopsies were evaluated when patients showed an ALT concentration more than twice the normal upper limit or at yearly intervals with informed consent. Biopsy specimens were evaluated by a single pathologist (H.H.) with extensive experience in the pathology of liver transplantation. Necro-inflammatory activity (A0–A3) and fibrosis stage (F0–F4) were assessed using the METAVIR score [24,25].

Statistical analysis

Baseline characteristics and Th subsets were recorded and compared between disease types. For continuous variables that were nearly symmetrically distributed, mean values and standard deviations (SDs) are given, and these data were analysed by *t*-test and one-way analysis of variance. For non-normally distributed variables, medians and ranges are given, and the data were analysed by the Wilcoxon and Kruskal–Wallis tests. For categorical variables, counts are given, and the data analysed by chi-square test. The rates of patients who showed a progression of fibrosis to stage F3 or F4 after initiation of the interferon therapy were estimated using the Kaplan–Meier method and compared using log-rank tests. A P value <0.05 was considered significant.

RESULTS

Biochemical cholestasis in patients with recurrent hepatitis C after LDLT

Eighty patients were diagnosed with recurrent HepC-LT and other aetiologies of liver injury were excluded by liver histology and imaging. The blood concentration of ALP and γ-GTP, enzymes that reflect cholestasis, of the 80 patients with HepC-LT was significantly higher than those of 103 patients with HepC-NT before interferon therapy. The median ALP level was 485.5 IU/L (range 204–2977) in HepC-LT patients, compared with 259 IU/L (range 121–772) in the HepC-NT group (P < 0.001). The median γ-GTP level was 148.5 IU/L (range 15–1827) in the HepC-LT group, compared with 41 IU/L (range 12–399) in the HepC-NT group (P < 0.001). We defined biochemical cholestasis as an ALP concentration more than 1.2 times (more than 431 IU/L) or a γ-GTP concentration more than four times (more than 216 IU/L for men and 116 IU/L for women) the upper limit of normal, because <10% of the patients in the HepC-NT group satisfied these criteria, showing remarkable difference between the HepC-LT and HepC-NT groups (Fig. 1). Of the 80 patients with HepC-LT, 48 patients (60%) had an ALP concentration more than 1.2 times the upper limit of normal, whereas only 5% of the HepC-NT group had a high ALP concentration. Thirty seven patients with HepC-LT (46%) had a γ-GTP concentration more than four times the upper limit of normal, whereas 6% of HepC-NT patients had a high γ-GTP concentration. Taken together, 69% of the patients with HepC-LT (55 patients) showed either a high ALP concentration (>1.2 times normal) or high γ-GTP concentration (>4 times normal), whereas only 9% of the patients in the HepC-NT group had high values for one of these variables. These data clearly show that biochemical cholestasis is a characteristic of HepC-LT.

The cause of the biochemical cholestasis in patients with HepC-LT was examined again by imaging and liver histology, retrospectively. Imaging by ultrasonography, CT, ERCP or MRCP, or a combination, did not reveal any causes of mechanical cholestasis, such as biliary obstruction. Analysis of liver histology demonstrated intrahepatic cholestasis only in 12 of 55 patients (22%) with biochemical cholestasis and in seven of 25 patients (28%) without cholestasis. The

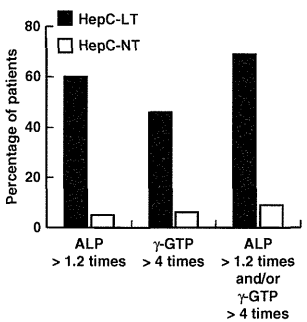

Fig. 1 Percentage of patients with biochemical cholestasis defined as increased serum alkaline phosphatase (ALP) concentration more than 1.2 times the upper limit of normal and/or gamma-glutamyl transpeptidase (γ-GTP) more than four times the upper limit of normal in patients with recurrent hepatitis C after liver transplantation (HepC-LT) or those with hepatitis C in non-transplant settings (HepC-NT).

prevalence and extension of liver steatosis also did not differ between patients with and without biochemical cholestasis. Steatosis, defined as more than 5% of hepatocytes with fat deposit on biopsy, was found in 22 of 55 patients (40%) with biochemical cholestasis, and in 11 of 25 patients (44%) without biochemical cholestasis. Thus, the major cause of biochemical cholestasis could not be determined by imaging or liver histology.

Progression of fibrosis in patients with biochemical cholestasis

As already mentioned, 55 (69%) of the 80 patients with HepC-LT showed biochemical cholestasis. These patients were classified into the cholestasis (Ch) group, and the remaining 25 patients (31%) were classified into the non-cholestasis (non-Ch) group. To evaluate the progression of liver injury in the Ch and non-Ch groups, we analysed the change in fibrosis stage by using the METAVIR score. The baseline fibrosis stages at diagnosis of recurrent hepatitis C did not differ between the Ch and non-Ch groups. The mean fibrosis stages were 0.95 in the Ch group (n = 55) and 1.06 in the non-Ch group (n = 25). We monitored the fibrosis stage by liver biopsy after initiation of interferon therapy at roughly yearly intervals. A liver biopsy was performed in 60 patients (75%) after the initiation of interferon therapy – including 43 in the Ch group (78%) and 17 in the non-Ch group (68%). The occurrence of fibrosis stage F3 or F4 in these 60 patients was assessed using Kaplan–Meier analysis (Fig. 2). No patient in the non-Ch group developed fibrosis stage F3 or F4, whereas 12 patients (28%) in the Ch group progressed to fibrosis stage F3 or F4 (P = 0.040, log-rank test). These data indicate that biochemical cholestasis was associated with the progression of fibrosis in the patients with HepC-LT.

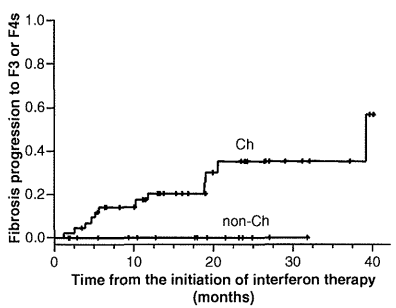

Fig. 2 Kaplan–Meier estimates of the rate of patients who showed progression of fibrosis to stage F3 or F4 (METAVIR score) after initiation of interferon therapy in patients with cholestasis (Ch) and without (non-Ch).

Effect of interferon therapy on biochemical cholestasis

To clarify the clinical characteristics of biochemical cholestasis in the patients with HepC-LT, we analysed the efficacy of interferon therapy in treating cholestasis (Fig. 3). Of the 55 Ch patients, 39 (71%) showed a virological response (VR) after interferon therapy, which was defined as a decrease in serum HCV RNA titre to <5 kIU/mL or a 2 $\log_{10}$ decrease. On the other hand, of the 25 non-Ch patients, 14 (56%) showed a VR following interferon therapy. When both ALP and γ-GTP concentrations decreased to the normal range or to less than half of the concentration before interferon therapy along with a reduced serum HCV RNA titre, cholestasis was assumed to be caused by HCV; we defined these patients as biochemical responders for cholestasis (Ch-VR-BR). Twenty two of the 39 (56%) virological responders with cholestasis satisfied these criteria and were classified into the Ch-VR-BR group. The biochemical cholestasis in the other 17 patients (44%) did not improve after interferon therapy despite a VR; these patients were classified into the Ch-VR-non-BR group. The lack of improvement indicated the presence of other mechanisms for development of cholestasis, although the imaging and histology could not

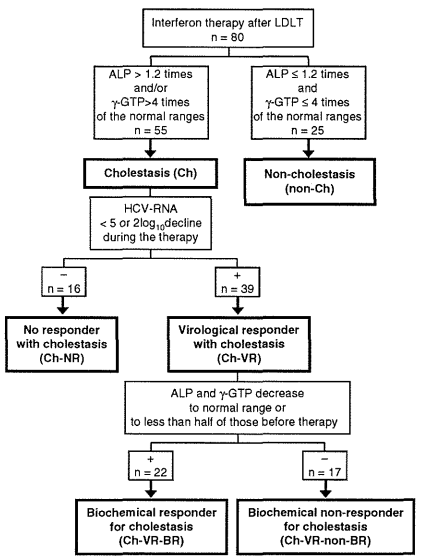

Fig. 3 Flow diagram showing the classification of patients with or without biochemical cholestasis, and the outcome of interferon therapy in patients with recurrent hepatitis C after liver transplantation. n = number of patients.

identify these causes before interferon therapy. However, after the initiation of interferon therapy, we found biliary obstruction in five patients and chronic rejection in three patients in the 17 patients with the Ch-VR-non-BR, suggesting that these conditions had caused the biochemical cholestasis. The causes of biochemical cholestasis in the remaining nine patients were unknown. Consequently, after excluding those eight patients, more than half of the cholestasis in patients with Ch-VR (22 patients of 31 patients) were interferon sensitive, indicating that cholestasis was attributed to HCV infection in the 22 patients. Based on the presence of biochemical cholestasis and the efficacy of interferon therapy, we classified the patients as shown in Fig. 3.

Increased Th1 responses in biochemical responders with cholestasis

Next, helper T-cell (Th) subsets of the peripheral blood were measured in the patients with HepC-LT by intracellular cytokine staining and flow cytometry, because Th responses are known to be an important factor for the progression of HepC-NT [26,27]. Peripheral blood cells were taken before interferon therapy from 18 patients with Ch, including nine patients with Ch-VR-BR, four with Ch-VR-non-BR and five with Ch-NR. Nine patients without cholestasis (non-Ch) were also analysed (Table 1). The percentage of Th1 cells and the Th1/Th2 ratio were significantly higher in the Ch than the non-Ch group ($P = 0.003$, t-test, and $P = 0.007$, Wilcoxon test respectively), suggesting that the increased Th1 response was associated with the cholestasis in the patients with HepC-LT. Then, to clarify the features of VR-Ch-BR that characterize cholestatic hepatitis caused by HCV, we compared the Th subsets among the Ch-VR-BR, Ch-VR-non-BR and non-Ch groups. As the Ch-NR group consisted of both HCV-related cholestasis and HCV-unrelated cholestasis, we excluded the Ch-NR group from the analysis. The percentage of Th1 cells was significantly higher in the Ch-VR-BR group than in Ch-VR-non-BR and non-Ch groups ($P = 0.001$, one-way analysis of variance). The percentage of Th0-DN cells in the Ch-VR-BR group was significantly lower than the other two groups ($P = 0.004$, Kruskal–Wallis test), but the percentages of Th2 cells and Th0-DP did not differ among the three groups, indicating pronounced differentiation of Th0-DN cells into Th1 cells in the Ch-VR-BR patients. Thus, this increased Th1 response in cholestatic patients with a biochemical response after interferon therapy suggests that cholestasis caused by HCV is associated with such a Th1 response.

DISCUSSION

In this study, we found that biochemical cholestasis, defined as a high ALP or γ-GTP concentration, was a characteristic feature of HepC-LT, and the biochemical cholestasis improved after interferon therapy in more than half of the patients. Differences of the clinical course between the HepC-LT and HepC-NT groups have been well documented. Rapid progression and poorer prognosis are well-known characteristics of HepC-LT compared with HepC-NT [8]. However, the differences in baseline characteristics have not been previously reported. Our data show that high ALP and/or γ-GTP concentration is a characteristic of HepC-LT that distinguishes it from the HepC-NT setting. This may not be surprising because several conditions related to transplantation, such as drug use, acute cellular rejection, chronic rejection, liver steatosis or biliary obstruction, result in cholestasis after liver transplantation. We excluded these conditions by liver histology and imaging, and then started interferon therapy for hepatitis C. Interestingly, after interferon therapy, the biochemical cholestasis improved in more than half of the patients in association with a reduction in HCV RNA titre, whereas no virological non-responder showed an improvement in biochemical cholestasis, indicating that the biochemical cholestasis was caused by HCV in many patients.

Table 1 Helper T-cell subsets in peripheral blood of patients with cholestasis (Ch) and without (non-Ch), and the three subgroups in the Ch group; biochemical responders for cholestasis (VR-Ch-BR), biochemical non-responders for cholestasis (VR-Ch-non-BR) in virological responders and virological non-responders (Ch-NR) before interferon therapy

	Ch				
	Total ($n = 18$)	Ch-VR-BR ($n = 9$)	Ch-VR-non-BR ($n = 4$)	Ch-NR ($n = 5$)	Non-Ch ($n = 9$)
Th1 (%)*	47.3‡ (13.1)	52.6¶ (11.9)	36.4 (11.6)	46.3 (12.6)	32.1 (6.5)
Th2 (%)*	1.28 (0.79)	1.41 (0.99)	1.20 (0.22)	1.12 (0.75)	1.86 (0.88)
Th0-DP (%)†	2.5 (0.7–14.9)	2.3 (0.7–14.9)	2.2 (1.6–2.5)	4.2 (2.4–7.6)	1.9 (0.8–7.4)
Th0-DN (%)†	46.2 (24.0–70.9)	44.6** (24–59.3)	62.3 (46–70.9)	41.2 (36.5–65.5)	60.9 (51.6–73.7)
Th1/Th2†	38.9§ (15.4–374)	38.8 (15.4–374)	25.3 (23.3–51.2)	42.6 (39.0–108.2)	16.9 (6.0–36.8)

Th0-DP, double-positive Th0; Th0-DN, double-negative Th0. *Mean (standard deviation). †Median (range). ‡Significantly higher than the non-Ch group ($P = 0.003$). §Significantly higher than the non-Ch group ($P = 0.007$). ¶Significantly higher than the Ch-VR-non-BR and the non-Ch groups ($P = 0.001$). **Significantly lower than the Ch-VR-non-BR and the non-Ch groups ($P = 0.004$).

This study also demonstrated that the biochemical cholestasis in the patients with HepC-LT is associated with the progression of liver fibrosis. However, we still do not know whether the biochemical cholestasis is related to FCH. Fibrosis is accelerated in patients with biochemical cholestasis, but the liver histology in our patients did not show the features of FCH. In the 80 patients with HepC-LT in this study, only two (2.5%) were diagnosed as having FCH by liver histology. Both patients with FCH were in the Ch-NR group. Previous reports showed 7–15% incidence [12–14] of FCH in patients with HCV after liver transplantation. The lower incidence in our study might indicate that interferon therapy has a role in inhibiting the progression to FCH.

We found that biochemical cholestasis in patients with HepC-LT is characterized by Th1 predominance. We also demonstrated that virological responders to interferon therapy who showed improvement in cholestasis (Ch-VR-BR) had a higher Th1 response than those without improvement in cholestasis (Ch-VR-non-BR) or those without cholestasis (non-Ch), suggesting that a Th1/Th2 profile is associated with the pathophysiology of HCV-induced cholestasis after liver transplantation. The host immune response plays a critical role in both the control of HCV replication and liver injury [26,27]. In particular, the $CD4^+$ T-cell responses to HCV play a key role in the outcome of the infection, and an imbalance between Th1 and Th2 cytokines has been suggested as a factor influencing the activity and progression of hepatitis C [28–31]. Indeed, a correlation between dominant Th1 responses and progression of chronic hepatitis C has been reported [31], suggesting that the Th1 response plays a role in accelerating the disease. Thus, the increased Th1 response in patients with cholestasis may be associated with a more severe progression of fibrosis in patients with cholestasis than in those without after liver transplantation. Although the precise mechanism is unknown at present, our results indicate that the higher Th1 response may be a good marker for determining the cause of cholestasis and predicting the efficacy of interferon therapy in terms of cholestasis for patients with recurrent HepC-LT. Patients with a higher Th1/Th2 ratio may be good candidates for receiving interferon therapy.

In conclusion, biochemical cholestasis is a characteristic feature in patients with HepC-LT, which is associated with progression of fibrosis. The improvement of biochemical cholestasis following antiviral therapy appears to be important in preventing this progression. An increased Th1 response to HCV may contribute to the pathophysiology of cholestasis caused by HCV and the rapid progression of HepC-LT. Thus, manipulation of the T-cell response may be a promising therapeutic approach for preventing progression of HepC-LT.

ACKNOWLEDGEMENT

This work was supported by Grants-in-aid for Scientific Research 19790480 from the Ministry of Education, Culture, Sports, Science and Technology of Japan.

REFERENCES

1 Berenguer M, Prieto M, San Juan F *et al.* Contribution of donor age to the recent decrease in patient survival among HCV-infected liver transplant recipients. *Hepatology* 2002; 36(1): 202–210.
2 Feray C, Caccamo L, Alexander GJ *et al.* European collaborative study on factors influencing outcome after liver transplantation for hepatitis C. European Concerted Action on Viral Hepatitis (EUROHEP) Group. *Gastroenterology* 1999; 117(3): 619–625.
3 Forman LM, Lewis JD, Berlin JA, Feldman HI, Lucey MR. The association between hepatitis C infection and survival after orthotopic liver transplantation. *Gastroenterology* 2002; 122(4): 889–896.
4 Gane E. The natural history and outcome of liver transplantation in hepatitis C virus-infected recipients. *Liver Transpl* 2003; 9(11): S28–S34.
5 Prieto M, Berenguer M, Rayon JM *et al.* High incidence of allograft cirrhosis in hepatitis C virus genotype 1b infection following transplantation: relationship with rejection episodes. *Hepatology* 1999; 29(1): 250–256.
6 Sanchez-Fueyo A, Restrepo JC, Quinto L *et al.* Impact of the recurrence of hepatitis C virus infection after liver transplantation on the long-term viability of the graft. *Transplantation* 2002; 73(1): 56–63.
7 Velidedeoglu E, Mange KC, Frank A *et al.* Factors differentially correlated with the outcome of liver transplantation in hcv+ and HCV- recipients. *Transplantation* 2004; 77(12): 1834–1842.
8 Berenguer M, Ferrell L, Watson J *et al.* HCV-related fibrosis progression following liver transplantation: increase in recent years. *J Hepatol* 2000; 32(4): 673–684.
9 Kuo A, Terrault NA. Management of hepatitis C in liver transplant recipients. *Am J Transplant* 2006; 6(3): 449–458.
10 Wiesner RH, Sorrell M, Villamil F. Report of the first International Liver Transplantation Society expert panel consensus conference on liver transplantation and hepatitis C. *Liver Transpl* 2003; 9(11): S1–S9.
11 Iacob S, Cicinnati VR, Hilgard P *et al.* Predictors of graft and patient survival in hepatitis C virus (HCV) recipients: model to predict HCV cirrhosis after liver transplantation. *Transplantation* 2007; 84(1): 56–63.
12 Cotler SJ, Taylor SL, Gretch DR *et al.* Hyperbilirubinemia and cholestatic liver injury in hepatitis C-infected liver transplant recipients. *Am J Gastroenterol* 2000; 95(3): 753–759.
13 Dickson RC, Caldwell SH, Ishitani MB *et al.* Clinical and histologic patterns of early graft failure due to recurrnet hepatitis C in four patients after liver transplantation. *Transplantation* 1996; 61(5): 701–705.
14 Schluger LK, Sheiner PA, Thung SN *et al.* Severe recurrent cholestatic hepatitis C following orthotopic liver transplantation. *Hepatology* 1996; 23(5): 971–976.

15 Ong JP, Younossi ZM, Gramlich T *et al.* Interferon alpha 2B and ribavirin in severe recurrent cholestatic hepatitis C. *Transplantation* 2001; 71(10): 1486–1487.
16 Cavicchi M, Beau P, Crenn P, Degott C, Messing B. Prevalence of liver disease and contributing factors in patients receiving home parenteral nutrition for permanent intestinal failure. *Ann Intern Med* 2000; 132(7): 525–532.
17 Lloyd DA, Zabron AA, Gabe SM. Chronic biochemical cholestasis in patients receiving home parenteral nutrition: prevalence and predisposing factors. *Aliment Pharmacol Ther* 2008; 27(7): 552–560.
18 Kumar KS, Saboorian MH, Lee WM. Cholestatic presentation of chronic hepatitis C: a clinical and histological study with a review of the literature. *Dig Dis Sci* 2001; 46(10): 2066–2073.
19 Takada Y, Haga H, Ito T *et al.* Clinical outcomes of living donor liver transplantation for hepatitis C virus (HCV)-positive patients. *Transplantation* 2006; 81(3): 350–354.
20 Ueda Y, Takada Y, Haga H *et al.* Limited benefit of biochemical response to combination therapy for patients with recurrent hepatitis C after living-donor liver transplantation. *Transplantation* 2008; 85(6): 855–862.
21 Ohno O, Mizokami M, Wu RR *et al.* New hepatitis C virus (HCV) genotyping system that allows for identification of HCV genotypes 1a, 1b, 2a, 2b, 3a, 3b, 4, 5a, and 6a. *J Clin Microbiol* 1997; 35(1): 201–207.
22 Morinobu A, Kumagai S. [Cytokine measurement at a single-cell level to analyze human Th1 and Th2 cells]. *Rinsho Byori.* 1998; 46(9): 908–914.
23 Schauer U, Jung T, Krug N, Frew A. Measurement of intracellular cytokines. *Immunol Today* 1996; 17(7): 305–306.
24 Bedossa P, Poynard T. An algorithm for the grading of activity in chronic hepatitis C. The METAVIR Cooperative Study Group. *Hepatology* 1996; 24(2): 289–293.
25 Poynard T, Bedossa P, Opolon P. Natural history of liver fibrosis progression in patients with chronic hepatitis C. The OBSVIRC, METAVIR, CLINIVIR, and DOSVIRC groups. *Lancet* 1997; 349(9055): 825–832.
26 Cerny A, Chisari FV. Pathogenesis of chronic hepatitis C: immunological features of hepatic injury and viral persistence. *Hepatology* 1999; 30(3): 595–601.
27 Diepolder HM, Zachoval R, Hoffmann RM, Jung MC, Gerlach T, Pape GR. The role of hepatitis C virus specific CD4 + T lymphocytes in acute and chronic hepatitis C. *J Mol Med* 1996; 74(10): 583–588.
28 Gerlach JT, Diepolder HM, Jung MC *et al.* Recurrence of hepatitis C virus after loss of virus-specific CD4(+) T-cell response in acute hepatitis C. *Gastroenterology* 1999; 117(4): 933–941.
29 Kamal SM, Rasenack JW, Bianchi L *et al.* Acute hepatitis C without and with schistosomiasis: correlation with hepatitis C-specific CD4(+) T-cell and cytokine response. *Gastroenterology* 2001; 121(3): 646–656.
30 Sarih M, Bouchrit N, Benslimane A. Different cytokine profiles of peripheral blood mononuclear cells from patients with persistent and self-limited hepatitis C virus infection. *Immunol Lett* 2000; 74(2): 117–120.
31 Sobue S, Nomura T, Ishikawa T *et al.* Th1/Th2 cytokine profiles and their relationship to clinical features in patients with chronic hepatitis C virus infection. *J Gastroenterol* 2001; 36(8): 544–551.

Cell Host & Microbe
Article

The Ubiquitin Ligase Riplet Is Essential for RIG-I-Dependent Innate Immune Responses to RNA Virus Infection

Hiroyuki Oshiumi,[1,*] Moeko Miyashita,[1] Naokazu Inoue,[2] Masaru Okabe,[2] Misako Matsumoto,[1] and Tsukasa Seya[1]
[1]Department of Microbiology and Immunology, Graduate School of Medicine, Hokkaido University, Kita-15, Nishi-7, Kita-ku Sapporo 060-8638, Japan
[2]Research Institute for Microbial Diseases, Osaka University, 3-1 Yamadaoka, Suita, Osaka 565-0871, Japan
*Correspondence: oshiumi@med.hokudai.ac.jp
DOI 10.1016/j.chom.2010.11.008

SUMMARY

RNA virus infection is recognized by the RIG-I-like receptors RIG-I and MDA5, which induce antiviral responses including the production of type I interferons (IFNs) and proinflammatory cytokines. RIG-I is regulated by Lys63-linked polyubiquitination, and three E3 ubiquitin ligases, RNF125, TRIM25, and Riplet, are reported to target RIG-I for ubiquitination. To examine the importance of Riplet in vivo, we generated Riplet-deficient mice. Fibroblasts, macrophages, and conventional dendritic cells from Riplet-deficient animals were defective for the production of IFN and other cytokines in response to infection with several RNA viruses. However, Riplet was dispensable for the production of IFN in response to B-DNA and DNA virus infection. Riplet deficiency abolished RIG-I activation during RNA virus infection, and the mutant mice were more susceptible to vesicular stomatitis virus infection than wild-type mice. These data indicate that Riplet is essential for regulating RIG-I-mediated innate immune response against RNA virus infection in vivo.

INTRODUCTION

RNA virus infection is initially recognized by RIG-I-like receptors, RIG-I and MDA5, which induce antiviral responses such as the production of type I interferons (IFNs) and proinflammatory cytokines (Yoneyama and Fujita, 2009; Takeuchi and Akira, 2010). Analyses of RIG-I and MDA5 knockout mice showed that RIG-I is essential for type I IFN production by mouse embryonic fibroblasts (MEFs), conventional dendritic cells (cDCs), and macrophages (Mfs) in response to RNA viruses such as vesicular stomatitis virus (VSV), influenza A virus (Flu), hepatitis C virus (HCV), Sendai virus (SeV), and Japanese encephalitis virus (JEV). MDA5 is critical in picornavirus infection (Kato et al., 2006; Saito et al., 2007). However, in plasmacytoid DCs (pDCs), loss of RIG-I has no effect on viral induction of IFNs, and TLR7 and MyD88 are required for inducing immune responses in these cells (Diebold et al., 2004; Kato et al., 2005; Kumar et al., 2006; Sun et al., 2006).

RIG-I consists of two N-terminal CARDs, a central DExD/H helicase domain, and a C-terminal repressor domain (CTD) (Yoneyama et al., 2004). Before viral infection, CTD of RIG-I suppresses N-terminal CARDs (Saito et al., 2007). When the CTD of RIG-I recognizes the 5′ triphosphate-double-stranded (ds) viral RNA, the conformation of the RIG-I protein changes, and the N-terminal CARD triggers interaction with its downstream partner IPS-1 (Hornung et al., 2006; Pichlmair et al., 2006; Saito et al., 2007; Cui et al., 2008; Takahasi et al., 2008; Rehwinkel et al., 2010). IPS-1 contains an N-terminal CARD that interacts with the tandem CARDs of RIG-I and a C-terminal transmembrane domain that localizes it to the mitochondrial outer membrane (Kawai et al., 2005; Meylan et al., 2005; Seth et al., 2005; Xu et al., 2005). IPS-1 activates TBK1 kinase, which mediates phosphorylation of IRF-3, leading to its dimerization and translocation into the nucleus (Kumar et al., 2006; Sun et al., 2006). The IRF-3 dimers, NF-κB, and AP-1 transcription factors activate type I IFN transcription (Honda et al., 2005). The secreted type I IFNs activates the IFNAR, which leads to phosphorylation and nuclear translocation of STAT1 (Akira et al., 2006; Honda et al., 2006).

RIG-I is regulated by ubiquitination. Three E3 ubiquitin ligases, RNF125, TRIM25, and Riplet, target RIG-I (Arimoto et al., 2007; Gack et al., 2007; Oshiumi et al., 2009). RNF125 functions as a negative regulator for RIG-I signaling and mediates Lys48-linked polyubiquitination of RIG-I, leading to protein degradation by the proteasome (Arimoto et al., 2007). On the other hand, TRIM25 and Riplet function as positive regulators for the signaling. TRIM25 mediates Lys63-linked polyubiquitination at Lys172 of RIG-I CARDs (Gack et al., 2007). Lys63-linked polyubiquitination induces interaction between RIG-I and IPS-1 CARDs, leading to the activation of signaling (Gack et al., 2007, 2008). However, there are several reports that describe other models. First, Zeng et al. developed an in vitro reconstitution system of the RIG-I pathway (Zeng et al., 2010). Using this system, they showed that Lys172 of RIG-I CARDs is required for binding to the Lys63-linked polyubiquitin chain (Zeng et al., 2010). They postulated that polyubiquitin binding and not ubiquitin modification is required for RIG-I activation (Zeng et al., 2010). In their model, unanchored polyubiquitin chains are responsible for RIG-I activation. However, they did not rule out the possibility that ubiquitination of some signaling proteins may contribute to RIG-I activation (Zeng et al., 2010). Second, Fujita T and his colleagues reported that residue 172 of mouse RIG-I is not Lys but Gln and human RIG-I K172R mutant was normally activated by SeV infection in RIG-I KO MEFs (Shigemoto et al., 2009).

The third ubiquitin ligase, Riplet, mediates Lys63-linked polyubiquitination of RIG-I CTD and CARDs (Gao et al., 2009; Oshiumi et al., 2009). This polyubiquitination promotes RIG-I activation and its antiviral activity in human cells (Horner and Gale, 2009; Nakhaei et al., 2009; Takeuchi and Akira, 2010; Yoneyama and Fujita, 2010); however, in vivo evidence is absent. Type I IFNs are mainly produced by DCs or Mf in vivo, and RIG-I is essential for type I IFN production in cDC and Mf (Kato et al., 2005; Sun et al., 2006; Kumagai et al., 2007). The role of Riplet in these cells also has not yet been examined. Both TRIM25 and Riplet proteins mediate Lys63-linked polyubiquitination of RIG-I, and thus Gao et al. suggested that Riplet may be a complementary factor of TRIM25 for RIG-I activation (Gao et al., 2009). Therefore, it is not known whether Riplet is essential for RIG-I activation. To address these issues, we generated Riplet knockout mice. Our analysis revealed that Riplet is essential for the RIG-I activation and innate immune responses against viral infection in vivo.

RESULTS

Ubiquitous Expression of Riplet mRNA

First, we examined mouse Riplet mRNA expression by quantitative PCR (qPCR), and found it to be ubiquitously expressed in various tissues, MEFs, bone marrow-derived DCs (BM-DCs), and Mf (BM-Mf) (Figure 1A, left panel). Furthermore, we have previously shown that human Riplet mRNA is expressed in various tissues. When we examined the expression of Riplet mRNA in human DCs, it was observed in human DCs as in HeLa cells (Figure 1A, right panel). These data indicate that Riplet is expressed in various tissues and cells that are able to produce type I IFNs.

Generation of Riplet-Deficient Mice

Previously, we have shown that Riplet is a positive regulator for RIG-I-mediated signaling, and it mediates Lys63-linked polyubiquitination of RIG-I. However, the functional role of Riplet in vivo remains unclear. To investigate the role of Riplet in vivo, we generated Riplet-deficient (*Riplet*$^{-/-}$) mice by homologous recombination of embryonic stem cells (ESCs) (Figure 1B). We confirmed the target disruption of Riplet without deletion outside the targeted region (Figure 1C, and see Figures S1A and S1B available online). Riplet mRNA expression was abolished in *Riplet*$^{-/-}$ cells (Figures 1E and 1F), and the knockout of Riplet did not affect the expression of other genes, such as RIG-I, MDA5, IPS-1, TICAM-1, TLR3, and TRIM25, which are involved in type I IFN production (Figure 1F). The mutant mice were born at the Mendelian ratio from *Riplet*$^{+/-}$ parents (Figure 1D), and they developed and bred normally. These mice displayed no apparent abnormalities up to 7 months of age. Mutations in the human Riplet/RNF135 gene cause the overgrowth syndrome (Douglas et al., 2007). We did not observe any overgrowth phenotypes in *Riplet*$^{+/-}$ and *Riplet*$^{-/-}$ mice. Next, we examined the composition of CD4-, CD8-, CD11c-, and/or PDCA1-positive cells in the spleen, and found no difference between wild-type and *Riplet*$^{-/-}$ mice (Figures S1C and S1D). Induction of cDC from BM in the presence of GM-CSF was also normal in *Riplet*$^{-/-}$ mice (Figure S1E). Therefore, the mouse Riplet gene is dispensable for development.

Riplet$^{-/-}$ Embryonic Fibroblasts Are Defective in Innate Immune Responses against RNA Viruses

Riplet is a positive regulator for RIG-I-mediated signaling. In mouse fibroblast, VSV and Flu are mainly recognized by RIG-I (Kato et al., 2006). Furthermore HCV 3′UTR RNA is also recognized by RIG-I (Saito et al., 2008). Therefore, we first examined the expression of type I IFNs, IFN-inducible gene IP-10, and Ccl5 in MEFs after HCV 3′UTR dsRNA transfection or infection with VSV or Flu. The induction of mRNA of IFN-α2, -β, IP-10, and Ccl5 in response to VSV or Flu was abrogated in *Riplet*$^{-/-}$ MEFs (Figures 2A–2D). In addition, transfection of low concentration of HCV 3′UTR dsRNA (0.05–0.2 μg/well) also failed to upregulate IFN-α2, -β, and IFN-inducible genes in *Riplet*$^{-/-}$ MEFs (Figures 2A–2D).

Single-stranded (ss) RNA, which is synthesized by T7 RNA polymerase in vitro, induced lower IFN-β expression than dsRNA (Figure S2A). The induction of IFN-β mRNA by HCV 3′UTR ssRNA was also abolished in *Riplet*$^{-/-}$ MEFs (Figure S2A). Although the induction of IFN-β mRNA in response to VSV infection was abrogated in *Riplet*$^{-/-}$ MEFs even at high (moi = 5) or low multiplicities of infection (moi = 0.2 or 1), the induction of IFN-β mRNA in response to high concentration of HCV dsRNA (0.8 μg/well) was detected in *Riplet*$^{-/-}$ MEFs (Figures S2C–S2K). Therefore, RIG-I does not require Riplet function in the presence of large amounts of naked viral RNA in the cytoplasmic region.

Recently, Onoguchi et al. reported that type III IFN, IFN-λ, induction was RIG-I dependent during viral infection (Onoguchi et al., 2007). The induction of IFN-λ mRNA in response to VSV was also abrogated in *Riplet*$^{-/-}$ MEFs (Figure S2B).

Next, we examined type I IFNs or IL-6 levels in culture supernatants after viral infection or HCV 3′UTR RNA transfection (low concentration condition). The production of IFN-α, -β, and IL-6 in culture supernatants was abrogated in *Riplet*$^{-/-}$ MEFs (Figures 3A–3C). Next, we analyzed the contribution of Riplet to the antiviral response. When MEFs were infected with VSV at various mois, cytopathic effects (CPEs) were more severe in *Riplet*$^{-/-}$ than in wild-type MEFs (Figure 3D). These results demonstrate that Riplet plays a critical role in the elimination of RNA virus infection by induction of IFN responses.

Riplet Is Dispensable for the Production of Type I IFN Induced by B-DNA and HSV-1 Infection

Cytoplasmic B-form double-stranded DNA (dsDNA) stimulates the cells to induce type I IFNs and IFN-inducible genes (Ishii et al., 2006). TBK1 is required for type I IFN induction by dsDNA (Ishii et al., 2008). Although immortalized MEFs require RIG-I for type I IFNs production by dsDNA stimulation, primary MEFs do not require IPS-1, which is a RIG-I adaptor, for type I IFNs production by dsDNA (Kumar et al., 2006; Chiu et al., 2009). We examined the expression of IFN-β and IP-10 mRNA by dsDNA stimulation in primary wild-type and *Riplet*$^{-/-}$ MEFs. IFN-β and IP-10 mRNA were detected in *Riplet*$^{-/-}$ MEFs by dsDNA transfection similar to that detected in wild-type MEFs (Figures 4A and 4B).

Next, we examined IFN-β mRNA expression during infection with DNA virus, HSV-1. Wild-type and *Riplet*$^{-/-}$ MEFs were infected with HSV-1, and IFN-β mRNA expression was examined by RT-qPCR. IFN-β expression in *Riplet*$^{-/-}$ MEFs was comparable to that in wild-type MEFs (Figure 4C). Taken together, these

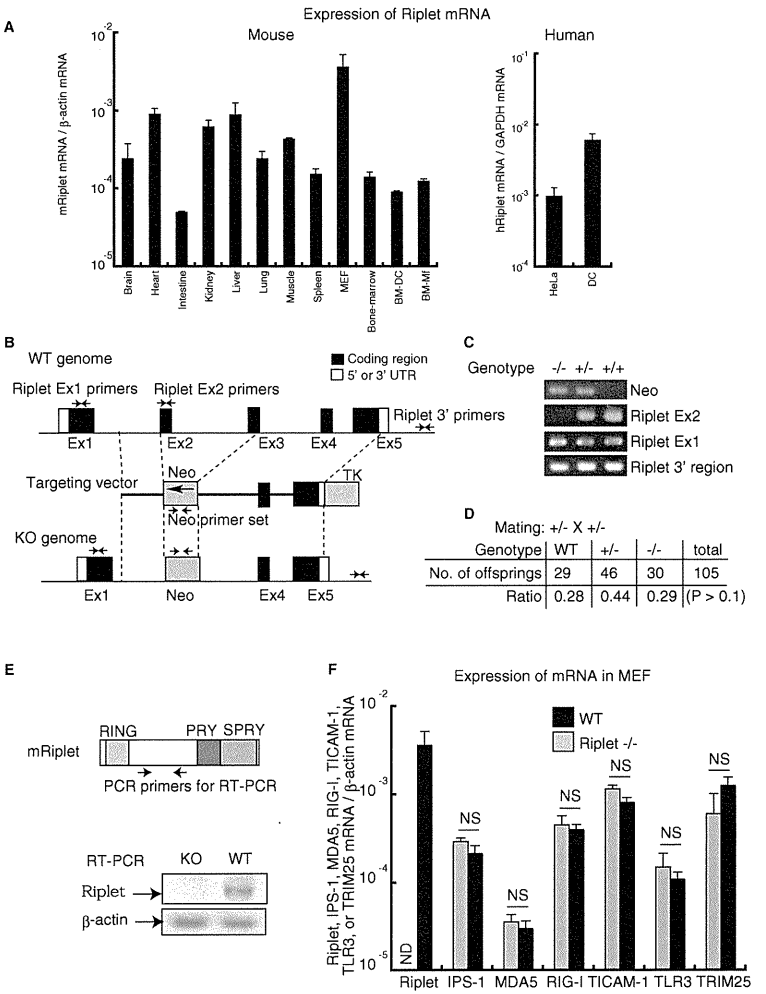

Figure 1. Targeted Disruption of the Murine Riplet Gene

(A) Riplet mRNA expression in mouse tissues and cells or human cells. RT-qPCR was performed to measure Riplet mRNA, and each sample was normalized to β-actin (mouse) or GAPDH (human). Data are shown as means ±SD and are representative of three independent experiments.

(B) Structure of the mouse Riplet gene, targeting vector, and disrupted gene. Closed boxes indicate the coding exon of Riplet, and hatched boxes indicate the Neo or TK gene coding region. The primer sets for PCR are shown by arrows.

data indicate that Riplet-dependent RIG-I activation is dispensable for type I IFN and IFN-inducible genes mRNA expression by cytoplasmic DNA in primary MEFs. This is consistent with previous studies reporting that the IPS-1-dependent pathway is dispensable for type I IFN production by cytoplasmic dsDNA stimulation (Kumar et al., 2006).

Riplet Is Essential for Triggering the RIG-I Signaling Pathway

We further examined the role of Riplet in RIG-I-mediated signaling during RNA virus infection. In RIG-I-mediated signaling, induction of type I IFNs and proinflammatory cytokines requires the activation of transcription factor IRF3. IRF3 is phosphorylated by TBK1 and IKK-ε. Phosphorylated IRF3 induces IFN-β gene expression. IFN-β produced subsequently stimulates the JAK-STAT pathway to amplify the responses. To determine the role of Riplet in signaling pathway activation, we analyzed IRF3 and STAT1 activations after VSV infection in *Riplet*$^{-/-}$ MEFs. VSV-induced dimerization of IRF3 and VSV- or Flu-induced pohsphorylation of STAT1 were abrogated in *Riplet*$^{-/-}$ MEFs (Figures 3E and 3F). These results demonstrate that Riplet is essential for activating the transcription factors that work early phase of RNA virus infection.

In the absence of viral infection, RIG-I CTD suppressed N-terminal CARDs (Saito et al., 2007). After viral infection, RIG-I CTD binds to viral RNA, leading to conformational changes (Saito et al., 2007). Later, RIG-I CARDs undergo TRIM25-mediated polyubiquitination and associate with IPS-1 CARD (Gack et al., 2007, 2008). When we tested the effect of Riplet on RIG-I activation, the full-length RIG-I protein with CTD failed to activate the IFN-β promoter in *Riplet*$^{-/-}$ MEFs (Figure 5A); however, promoter activation by the expression of RIG-I CARDs without CTD was normal in *Riplet*$^{-/-}$ MEFs (Figure 5B). These data indicate that Riplet is required for the activation of full-length RIG-I, but not for the activation of RIG-I CARDs without CTD. Next, we performed complementation assays. Immortalized *Riplet*$^{-/-}$ MEFs were transfected with an empty-, RIG-I-, or RIG-I-5KA mutant-expressing vector together with or without Riplet-expressing vector. The RIG-I-5KA mutant harbors mutations in five C-terminal Lys residues that are important for Riplet-mediated ubiquitination (Oshiumi et al., 2009). In the *Riplet*$^{-/-}$ cell line, RIG-I was not activated by HCV RNA stimulation, and Riplet expression led to the activation of wild-type RIG-I (Figure 5C). The deletion of the Riplet RING finger domain, which is the catalytic domain of ubiquitin ligase, abolished RIG-I activation (Figure 5D). Unlike wild-type RIG-I, Riplet expression failed to activate the RIG-I-5KA mutant protein (Figure 5C). The activations of wild-type and mutant RIG-I were correlated with its polyubiquitination (Figure S3A). Although the RNA binding activity was weakly reduced by the 5KA mutation, the pull-down assay showed that RIG-I-5KA mutant bound to dsRNA (Figure S3B). Next, we examined ligand-independent RIG-I activation by overexpression of Riplet. Overexpression of Riplet in HEK293 cells activated RIG-I in the absence of RIG-I ligand, such as viral RNA (Figure S3C). This ligand-independent activation of RIG-I by Riplet overexpression was also abolished by the 5KA mutation (Figure S3C). In addition, we examined the polyubiquitination of exogenously expressed RIG-I CTD fragment. Polyubiquitination of RIG-I CTD fragment was increased by overexpression of Riplet (Figure 5M), and was reduced by overexpression of the dominant-negative form of Riplet (Riplet DN) (Figure 5N). Polyubiquitination of RIG-I CTD fragment was not detected in Riplet-deficient cells (R3T cells); however, expression of Riplet led to polyubiquitination of RIG-I CTD fragment (Figure 5O). These data are consistent with our previous report (Oshiumi et al., 2009). Taken together, these data indicate that Riplet-dependent polyubiquitination of RIG-I is important for RIG-I activation.

Previously, we showed that Riplet is not involved in MDA5-mediated signaling. IFN-β promoter activation by MDA5 overexpression was normal in *Riplet*$^{-/-}$ MEFs (Figure 5E). Transfection of poly(I:C), which is recognized by MDA5, induced IFN-β, IL-6, and IP-10 expression in both wild-type and *Riplet*$^{-/-}$ MEFs (Figures 5F–5H). In addition, stimulation with lipopolysaccharide (LPS), which is a TLR4 ligand, normally induced expression of these cytokines in *Riplet*$^{-/-}$ MEFs (Figures 5I–5K). Furthermore, IL-6 production in culture medium in response to LPS was normal in *Riplet*$^{-/-}$ MEFs (Figure 5L). Taken together, these data indicate that Riplet is essential for the RIG-I-mediated type I IFN or IL-6 production upon viral infection in nonprofessional immune cells like fibroblasts, but is not required for MDA5- or TLR4-mediated signaling.

Riplet Is Required for Antiviral Innate Immune Responses in Conventional Dendritic Cells and Macrophages

We examined whether Riplet is required for the induction of type I IFN in DCs or Mf. DCs play a pivotal role in bridging innate and adaptive immune responses, and can be classified into cDCs and pDCs, the latter producing high levels of type I IFNs. Mfs also produce type I IFN. We induced cDCs from BM cells in the presence of GM-CSF (BM-DC). Twenty-four hours after VSV or Flu infection, cDCs of wild-type mice produced IFN-α, -β, and IL-6 (Figures 6A–6F). In contrast, the cDCs of *Riplet*$^{-/-}$ mice showed severely impaired IFN-α, -β, or IL-6 production during VSV or Flu infection (Figures 6A–6F). When the cDCs were stimulated with a TLR4 ligand, such as LPS, IFN-β or IL-6 production in *Riplet*$^{-/-}$ cDCs was almost normal (Figures S4A and S4B), indicating that Riplet is dispensable for LPS-induced cytokine production in cDCs.

Then we tested M-CSF-induced BM-Mf. Wild-type Mf produced IFN-α, -β, and IL-6 after VSV or Flu infection (Figures

(C) PCR of mouse tail. Genomic DNA was extracted from wild-type, *Riplet*$^{+/-}$, or *Riplet*$^{-/-}$ mice tails and PCR was performed using primers shown in (B).
(D) Genotype analyses of offspring from heterozygote intercrosses. Chi-square goodness-of-fit test indicated that deviation from Mendelian ratio was not statistically significant ($p > 0.1$).
(E) RT-PCR of MEFs. Total RNA from wild-type and *Riplet*$^{-/-}$ MEFs were extracted and subjected to RT-PCR to determine Riplet mRNA expression.
(F) Riplet, IPS-1 MDA5, RIG-I, TICAM-1, TLR3, and TRIM25 expression in MEFs. Total RNA from wild-type and *Riplet*$^{-/-}$ MEFs were extracted and subjected to RT-qPCR to determine mRNA expression. Expression of the indicated gene mRNA was normalized to β-actin mRNA expression. Data are shown as means ±SD and are representative of three independent experiments. "NS" indicates no statistically significant difference between the two samples.
See also Figure S1 and Table S1.

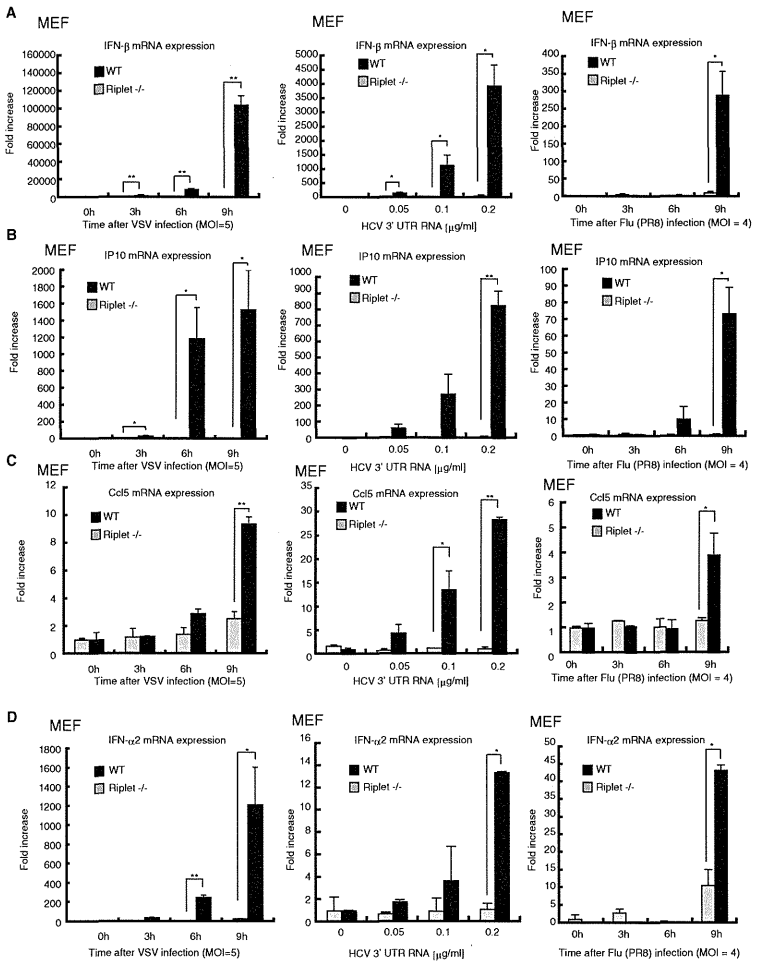

Figure 2. Abolished Responses to RNA Virus Infection in *Riplet*$^{-/-}$ Fibroblasts

Wild-type or *Riplet*$^{-/-}$ MEFs were infected with VSV or influenza A virus (Flu), and total RNA was extracted at the indicated times. Short HCV 3'UTR dsRNA was transfected into wild-type or *Riplet*$^{-/-}$ MEFs, and total RNA was extracted after 24 hr. Extracted RNA was subjected to RT-qPCR to determine IFN-β (A), IP10 (B), Ccl5 (C), or IFN-α2 (D) expression. Expression of each sample was normalized to β-actin mRNA expression. Data are shown as means ±SD and are representative of three independent experiments. *$p < 0.05$, **$p < 0.01$ (t test).
See also Figure S2 and Table S1.

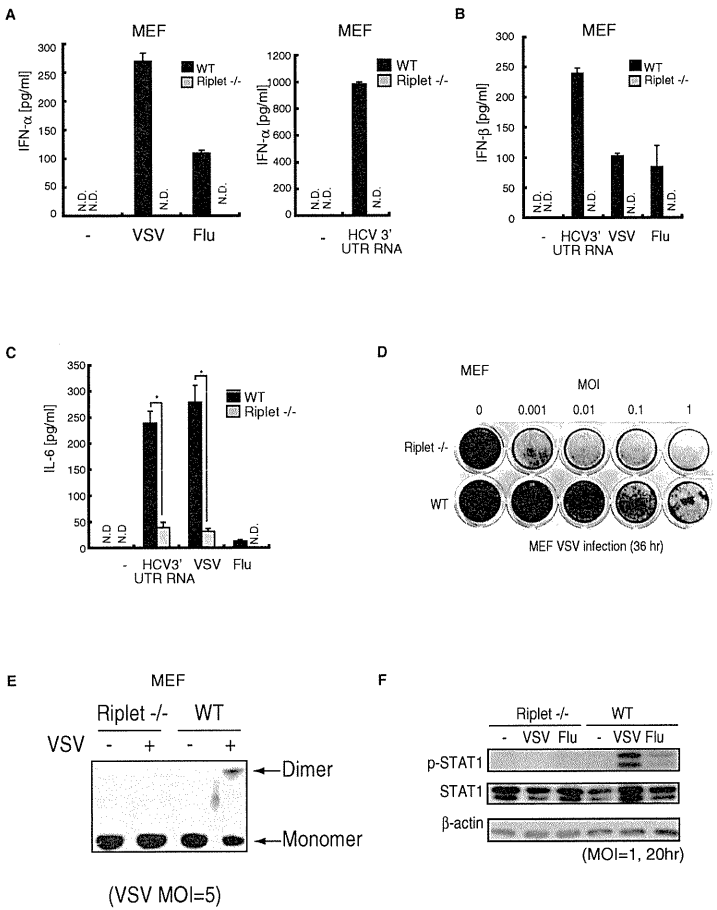

Figure 3. Role of Riplet in Antiviral Responses in Fibroblasts

(A–C) Wild-type or *Riplet*$^{-/-}$ MEFs were infected with VSV or Flu or transfected with short HCV 3′UTR dsRNA. Amounts of IFN-α (A), -β (B), and IL-6 (C) in culture supernatants were measured by ELISA after 24 hr. Data are shown as means ±SD and are representative of three independent experiments. *$p < 0.05$, **$p < 0.01$ (t test).

(D) Wild-type or *Riplet*$^{-/-}$ MEFs were infected with VSV at the indicated moi, and after 36 hr MEFs were fixed with formaldehyde and stained with crystal violet.

(E) Wild-type or *Riplet*$^{-/-}$ MEFs were infected with VSV at moi = 5, and after 9 hr cell lysates were prepared and analyzed by native PAGE. IRF-3 proteins were stained with anti-IRF3 antibody.

(F) Wild-type or *Riplet*$^{-/-}$ MEFs were infected with VSV or Flu at moi = 1, and after 20 hr cell lysates were prepared. The samples were analyzed by SDS-PAGE and western blotting. They were stained with anti-STAT1, phospho-STAT1, or β-actin antibodies.

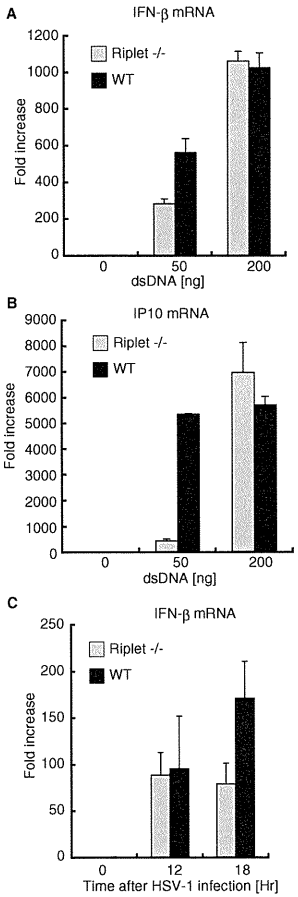

Figure 4. Role of Riplet in Type I IFN Production Induced by Cytoplasmic dsDNA

(A and B) Wild-type and *Riplet*$^{-/-}$ MEFs were transfected with the indicated amounts of dsDNA (Salomon sperm DNA) using the Lipofectamine 2000 reagent. Nine hours after the transfection, IFN-β (A) and IP-10 (B) mRNA expression was determined by RT-qPCR. Data are shown as means ±SD and are representative of three independent experiments.

(C) Wild-type and *Riplet*$^{-/-}$ MEFs were infected with HSV-1 at moi = 4, and IFN-β mRNA expression at the indicated times was examined by RT-qPCR. Data are shown as means ±SD and are representative of three independent experiments.

6A–6F). Similar to cDCs, cytokine production was reduced in Riplet knockout mice (Figures 6A–6F). Peritoneal Mf were isolated from wild-type and *Riplet*$^{-/-}$ mice. Knockout of Riplet reduced type I IFN production from peritoneal Mfs during VSV infection (Figures S4C and S4D).

We next generated Flt3L-induced DCs (Flt3L-DCs), which contain pDCs. Akira and his colleagues previously showed that the knockout of RIG-I or IPS-1 does not reduce type I IFN and IL-6 production by Flt3L-DCs, because RIG-I is dispensable for cytokine production in pDCs (Kato et al., 2005). The Flt3L-DCs of *Riplet*$^{-/-}$ mice produced normal amounts of IFN-a, -β, and IL-6 during Flu infection (Figures 6A–6F). This is consistent with the notion that Riplet is essential for the RIG-I-mediated type I IFNs and IL-6 production. Although the IFN-α levels in the culture medium after VSV infection were comparable with those in wild-type and *Riplet*$^{-/-}$ mice, Flt3L-DCs of *Riplet*$^{-/-}$ mice produced less IL-6 compared with that produced by wild-type mice through an unknown mechanism (Figure 6C).

Next, we examined type I IFN production during SeV infection. SeV infection induced IFN-α and -β productions from wild-type BM-DC, and the knockout of Riplet reduced IFN-α and -β productions from BM-DC (Figures S4E–S4J). Wild-type Flt3L-DC produced IFN-α after SeV infection, and the knockout of Riplet did not reduce IFN- α production from Flt3L-DC (Figures S4E–S4J).

Riplet Is Essential for Antiviral Immune Defense In Vivo

To investigate the role of Riplet in antiviral responses in vivo, wild-type and *Riplet*$^{-/-}$ mice were injected intraperitoneally with wild-type VSV, and sera were collected to measure type I IFN and IL-6 levels. IFN-α, -β, and IL-6 levels in sera were markedly reduced in *Riplet*$^{-/-}$ mice compared to in wild-type mice (Figures 7A and 7B, and Figure S5A). Next, wild-type and *Riplet*$^{-/-}$ mice were intranasally infected with VSV, and type I IFN levels in their sera were measured. At early time points, IFN-α and -β production was reduced in *Riplet*$^{-/-}$ mice compared to wild-type mice (Figures 7C and 7D); however, cytokine levels were comparable at later time points (Figures S5B and S5C). Previously, Ishikawa et al. observed that the knockout of STING gene, which is involved in RIG-I-dependent signaling, leads to reduction of type I IFN at early time points and relatively less reduction at later time points (Ishikawa and Barber, 2008; Ishikawa et al., 2009).

To determine if Riplet deficiency affects the survival of mice after VSV infection, the mice were intranasally infected with VSV, and their survival was monitored. Wild-type mice survived VSV infection; however, *Riplet*$^{-/-}$ mice were susceptible to VSV infection (Figure 7E). The viral titer in *Riplet*$^{-/-}$ mice brains 7 days after infection was higher than in wild-type mice (Figure 7F). These data indicate that Riplet plays a key role in the host defenses against VSV infection in vivo, and type I IFN production at early time points is important for host defenses.

DISCUSSION

In this study, we presented genetic evidence that Riplet is indispensable for antiviral responses in MEFs, BM-Mf, and BM-DCs, but not in Flt3L-DCs. The cell-type-specific requirement of Riplet

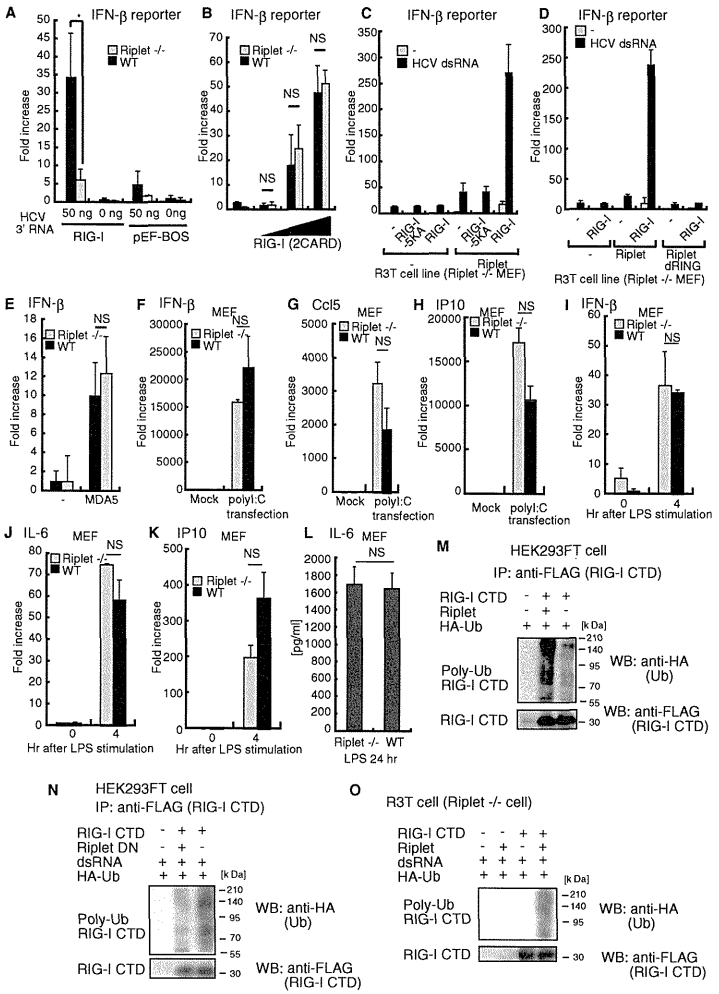

Figure 5. Role of Riplet in the RIG-I-Dependent Pathway

(A) Expression vector of full-length RIG-I and reporter plasmids were transfected into wild-type or *Riplet*$^{-/-}$ MEFs with or without HCV 3′UTR short dsRNA, and after 24 hr IFN-β promoter activation was examined by reporter gene assay. Data are shown as means ±SD and are representative of three independent experiments. *$p < 0.05$ (t test).

is similar to that of RIG-I. Previously, we showed that Riplet binds to RIG-I and mediates Lys63-linked polyubiquitination of RIG-I (Oshiumi et al., 2009). Genetic evidence in this study revealed that Riplet function is essential for RIG-I-dependent type I IFN production. Knockout of Riplet reduced type I IFN production in vivo during the early phase of VSV infection, and *Riplet*$^{-/-}$ mice were susceptible to VSV infection. Taken together, our results provide genetic evidence that Riplet is essential for RIG-I-dependent antiviral immune response in vivo. Most *RIG-I*$^{-/-}$ embryos were lethal at embryonic days 12.5–14.0 in some strain backgrounds (Kato et al., 2005). However, we could not observe any developmental defect in Riplet knockout mice as far as we examined.

Previously, Chen and his colleagues independently isolated Riplet and named it REUL (Gao et al., 2009). They reported that REUL/Riplet binds to RIG-I CARDs but not to CTD (Gao et al., 2009). Furthermore, they reported that REUL/Riplet mediates Lys63-linked polyubiquitination of Lys172 of RIG-I CARDs in a manner similar to TRIM25 (Gack et al., 2007; Gao et al., 2009). Although they did not show any expression profile data for Riplet and TRIM25, they mentioned that TRIM25 and Riplet have different distribution patterns, and thus hypothesized that REUL/Riplet is a complementary factor of TRIM25 and is required for RIG-I activation in cells that do not express TRIM25 (Gao et al., 2009). However, our genetic evidence is not consistent with their hypothesis, because Riplet is essential for RIG-I activation in MEFs that express TRIM25. Previously, Gack et al. showed that knockout of TRIM25 alone abolished RIG-I activation in MEFs (Gack et al., 2007). Therefore, null mutation in either Riplet or TRIM25 abolishes RIG-I activation. This genetic evidence indicates that Riplet can mediate polyubiquitination of RIG-I Lys residues that are not ubiquitinated by TRIM25. This means that Riplet functions differently than TRIM25 in RIG-I activation.

We isolated Riplet cDNA by yeast two-hybrid screening using the C-terminal region of RIG-I (Oshiumi et al., 2009). Because the yeast genome does not encode RIG-I, the interaction indicates the direct binding of Riplet to the RIG-I C-terminal region. The interaction between RIG-I CTD and Riplet has also been confirmed by immunoprecipitation assays in human cells (Oshiumi et al., 2009). Moreover, we have shown that Riplet expression leads to Lys63-linked polyubiquitination of RIG-I CTD (Oshiumi et al., 2009). Recently, Zheng et al. showed that RIG-I CARDs has the ability to bind to polyubiquitin chains (Zeng et al., 2010). We have carefully detected Riplet-mediated polyubiquitination of RIG-I C-terminal region without CARDs, under high-salt conditions, in which many protein-protein interactions were abolished (Oshiumi et al., 2009). Therefore, we proposed the hypothesis that Riplet mediates Lys63-linked polyubiquitination of RIG-I CTD (Oshiumi et al., 2009). This model can explain the genetic evidence that Riplet is essential for RIG-I activation in MEFs that express TRIM25. Gack et al. showed that K172R mutation alone caused near-complete loss of ubiquitination of the human RIG-I CARDs (Gack et al., 2007). Because residue 172 of mouse RIG-I is not Lys but Gln (Shigemoto et al., 2009), Riplet/Reul does not ubiquitinate residue 172 of mouse RIG-I. Based on the previous studies and our current data, we prefer the interpretation that Riplet activates RIG-I through polyubiquitination of RIG-I CTD. However, this interpretation does not exclude the possibility that Riplet ubiquitinates both CTD and CARDs of RIG-I (Gao et al., 2009; Oshiumi et al., 2009).

Previously, we showed that Lys849, -851, -888, -907, and -909 are critical residues in Riplet-mediated RIG-I CTD ubiquitination (Oshiumi et al., 2009). These five Lys residuse are close to the dsRNA binding sites of RIG-I CTD (Takahasi et al., 2008), and the 5KA mutation weakly reduced RNA binding activity of RIG-I. Therefore, it is possible that the 5KA mutation abrogate activation and polyubiquitination of RIG-I by reducing RNA biding activity of RIG-I. However, this possibility is weakened by following observations. First, the 5KA mutation caused near-complete loss of RIG-I activation, but the RIG-I-5KA mutant protein still possessed RNA binding activity. Second, overexpression of Riplet led to RIG-I activation in the absence of dsRNA in HEK293 cells, and this ligand-independent activation of RIG-I

(B) Expression vector for the two RIG-I N-terminal CARDs were transfected into wild-type or *Riplet*$^{-/-}$ MEFs together with reporter plasmids, and IFN-β promoter activation was examined by the reporter gene assay. Data are shown as means ±SD and are representative of three independent experiments. "NS" indicates not statistically significant.

(C) Empty, wild-type RIG-I-, or RIG-I-5KA mutant-expressing vectors were transfected into the *Riplet*$^{-/-}$ MEF cell line together with or without the Riplet-expressing vector. Cells were stimulated with HCV 3′UTR short dsRNA, and reporter gene assay was performed as described in (A).

(D) Empty or wild-type RIG-I-expressing vectors were transfected into the *Riplet*$^{-/-}$ MEF cell line together with empty, wild-type Riplet, or Riplet mutant (Riplet dRING)-expressing vector. Cells were stimulated with HCV 3′UTR short dsRNA, and the reporter gene assay was performed as described in (A).

(E) Empty or MDA5-expressing vectors was transfected into wild-type or *Riplet*$^{-/-}$ MEFs together with reporter plasmids, and after 24 hr IFN-β promoter activation was examined by the reporter gene assay.

(F–H) Of poly(I:C), 0.8 μg was transfected into wild-type or *Riplet*$^{-/-}$ MEFs. Twenty-four hours after transfection, total RNA was extracted from MEFs and subjected to RT-qPCR to determine IFN-β (F), Ccl5 (G), and IP10 (H) expression. Expression in each sample was normalized to the β-actin mRNA expression.

(I–K) Wild-type or *Riplet*$^{-/-}$ MEFs were stimulated with 1 μg of LPS. Total RNA was extracted at the indicated times and subjected to RT-qPCR analysis for of IFN-β (I), IL-6 (J), or IP-10 (K) expression.

(L) Wild-type or *Riplet*$^{-/-}$ MEFs were stimulated with LPS, and after 24 hr the amount of IL-6 in culture supernatants was measured by ELISA.

(M) HEK293FT cells were transfected with Riplet, FLAG-tagged RIG-I-CTD, and HA-tagged ubiquitin (HA-Ub) expression vectors. Twenty-four hours after transfection, cell lysates were extracted and immunoprecipitation was carried out with anti-FLAG antibody as previously described (Oshiumi et al., 2009). The samples were analyzed by SDS-PAGE, and western blotting was performed using anti-HA polyclonal antibody (Ub) and anit-Flag M2 monoclonal antibody (RIG-I-CTD). The plasmids are described previously (Oshiumi et al., 2009).

(N) Expression vector of dominant negative form of Riplet (Riplet DN) was transfected into HEK293FT cells together with expression vector of FLAG-tagged RIG-I CTD and HA-tagged ubiquitin. Cells were stimulated with dsRNA. Ubiquitination of RIG-I CTD was detected as in (M).

(O) R3T cells were transfected with Riplet, FLAG-tagged RIG-I-CTD, and HA-tagged ubiquitin (HA-Ub) expression vectors. Cells were stimulated with dsRNA. Ubiquitination of RIG-I-CTD was detected as in (M).

See also Figure S3.